

Excerpt lecture notes for doctoral training program 'QCD under extreme conditions'

**-The Functional Renormalization Group-
&
applications to gauge theories and gravity**

J. M. Pawłowski, J. A. Bonnet, S. Rechenberger

June 13, 2018

Contents

1	The Functional Renormalisation Group	3
1.1	Euclidean Quantum Field Theory	5
1.2	Dyson–Schwinger Equations	9
1.3	Renormalization	13
1.3.1	Perturbative Renormalization	13
1.3.2	Wilsonian Renormalization	17
1.4	Functional Renormalization Group Equations	21
1.5	Truncation schemes	29
1.5.1	Loop Expansion	29
1.5.2	Vertex Expansion	31
1.5.3	Derivative Expansion	32
1.5.4	Zero-Dimensional Toy Model	35
2	Appendix	39
2.1	Fourier Conventions	39
2.2	Wilsonian Renormalization for φ^4 theory	39
2.3	Local Potential Approximation of the $O(N)$ Model	41
2.4	Grassmann variables: Reminder	47
2.5	Flow equation of a four-Fermi coupling	48

1 The Functional Renormalisation Group

1.1 Euclidean Quantum Field Theory

A general QFT is fully determined by its complete set of correlation functions. As an illustrative example let us consider the simple case of a QFT with one real scalar field $\varphi(x)$ in d dimensions. This exemplary theory will be used frequently throughout this chapter, and its first few correlation or Green functions in a statistical approach in Euclidean spacetime are summarised in Table 1.1. These correlation functions of the fundamental quantum field φ are the moments of the central quantity in quantum statistical field theory, the generating functional $\mathcal{Z}[J]$. The latter is the analogue of the partition function in classical statistics and contains all information of the physical system under consideration. We obtain the correlation function in terms of the generating functional via functional derivatives as

$$\langle \varphi(x_1) \dots \varphi(x_n) \rangle_J = \frac{1}{\mathcal{Z}[J]} \frac{\delta^n \mathcal{Z}[J]}{\delta J(x_1) \dots \delta J(x_n)}. \quad (1.1)$$

Here the subscript J at the correlation function marks its dependence on the source field $J(x)$. The generating functional $\mathcal{Z}[J]$ can be given in terms of a path integral via

$$\mathcal{Z}[J] = \frac{1}{\mathcal{N}} \int [d\varphi]_{\text{ren}} \exp \left\{ -S[\varphi] + \int d^d x \varphi(x) J(x) \right\}, \quad (1.2)$$

with an exponential damping factor $\exp(-S[\varphi])$ with classical action $S[\varphi]$ and a flat measure $[d\varphi]_{\text{ren}}$. The subscript at the measure denotes the fact that in general such a path integral has to be regularised and renormalised. Note that the normalisation \mathcal{N} in front of the path integral drops out for correlation functions which is obvious from their definition in (1.1). Using this definition the correlation functions (1.1) are simply the normalised moments of the statistical integral (1.2).

Having a closer look at Table 1.1, e.g. the line $n = 2$, one realises that the two-point correlation function $\langle \varphi(x)\varphi(y) \rangle$ is written as a connected part, $\langle \varphi(x)\varphi(y) \rangle_{\text{connected}}$, and a disconnected one which reads $\phi(x)\phi(y) = \langle \varphi(x) \rangle \langle \varphi(y) \rangle$. The "connected" and "disconnected" refers to the classification in terms of the Feynman diagrams the correlation functions are built of. The disconnected part of a correlation function consists out of diagrams that decay in several subdiagrams that are not connected by lines. For example, the disconnected part of the two-point correlation function in Table 1.1 consists of the mean fields. Therefore its information is already stored in the one-point correlation function. The same is true for a general n -point correlation function whose disconnected part can be constructed from the connected parts of the m -point correlation functions, where $m < n$. Hence, $\mathcal{Z}[J]$ comprises redundant information. Within the Schwinger functional, $\mathcal{W}[J]$, part of this redundancy is removed. It is defined as

$$\mathcal{W}[J] = \ln \mathcal{Z}[J], \quad (1.3)$$

n	n -point correlation function		interpretation
0	$\langle 1 \rangle$	= 1	normalisation
1	$\langle \varphi(x) \rangle$	= $\phi(x)$	mean field
2	$\langle \varphi(x)\varphi(y) \rangle$	= $\langle \varphi(x)\varphi(y) \rangle_{\text{connected}} + \phi(x)\phi(y)$	propagator
3	$\langle \varphi(x)\varphi(y)\varphi(z) \rangle$	= $\langle \varphi(x)\varphi(y)\varphi(z) \rangle_{\text{connected}} + \dots$	three-point vertex
\vdots	\vdots	\vdots	\vdots

Table 1.1: The finite n -point correlation functions $\langle \varphi(x_1) \dots \varphi(x_n) \rangle$ ($n \in \mathbb{N}_0$) of a real scalar field theory with one scalar field $\varphi(x)$.

and serves as the generating functional for the connected correlation functions. As for the correlation functions, the connected correlation functions are independent of the normalisation \mathcal{N} in (1.2). This is simple to see as $-\ln \mathcal{N}$ is an additive constant in $\mathcal{W}[J]$. Henceforth we shall drop the normalisation. Moreover, $W[J]$ is a convex functional: its second derivative, the connected two-point function or propagator $G(x, y)$, is positive. This is easily seen from its definition

$$G(x, y) := \frac{\delta^2 W[J]}{\delta J(x) \delta J(y)} = \langle \varphi(x) \varphi(y) \rangle - \phi(x) \phi(y) = \langle (\varphi(x) - \langle \varphi(x) \rangle) (\varphi(y) - \langle \varphi(y) \rangle) \rangle. \quad (1.4)$$

Evaluated at $x = y$ the propagator $G(x, x)$ is the expectation value of a positive operator $(\varphi(x) - \langle \varphi(x) \rangle)^2$, which entails convexity of $W[J]$.

The Schwinger functional still contains redundant information, as connected correlation functions can be separated into one-particle irreducible (1PI) and one-particle reducible ones. The 1PI correlation functions contain the information of 1PI Feynman diagrams: 1PI diagrams can not be separated into two disconnected ones by cutting one internal line. General connected diagrams can be built from the 1PI diagrams, and hence the 1PI correlation functions contain all information about the QFT under consideration. The generating functional of 1PI correlation functions, the effective action $\Gamma[\phi]$, is the Legendre transform of the Schwinger functional,

$$\Gamma[\phi] = \sup_J \left\{ \int d^d x J(x) \phi(x) - \mathcal{W}[J] \right\}. \quad (1.5)$$

The Legendre transform $\Gamma[\phi]$ in (1.5) is convex as is the Schwinger functional $\mathcal{W}[J]$. Therefore, the Legendre transform of Γ is again W . The physics interpretation of the effective action is that of the quantum analogue of the classical action. The field ϕ in the effective action is indeed the mean field. This is easily seen by taking the derivative with respect to J of Eq. (1.5). In position space and momentum space we find ¹

$$\phi(x) = \left. \frac{\delta \mathcal{W}[J]}{\delta J(x)} \right|_{J_{\text{sup}}} = \frac{1}{\mathcal{Z}[J]} \left. \frac{\delta \mathcal{Z}[J]}{\delta J(x)} \right|_{J_{\text{sup}}} = \langle \varphi(x) \rangle, \quad \frac{\delta \mathcal{W}[J]}{\delta J(p)} = \phi(-p). \quad (1.6)$$

Here we inserted (1.3) and used the definition of the mean field as the one-point correlation function in (1.1). This relation defines the Legendre transform of $\delta \mathcal{W} / \delta J$. Analogously, the Legendre transform of $\delta \Gamma / \delta \phi$ can be obtained by taking the functional derivative of (1.5) with respect to ϕ . The result in position space and momentum space reads

$$\frac{\delta \Gamma[\phi]}{\delta \phi(x)} = J_{\text{sup}}(x), \quad \frac{\delta \Gamma[\phi]}{\delta \phi(p)} = J_{\text{sup}}(-p). \quad (1.7)$$

These are the quantum equations of motion (EoM). Notably, for vanishing J_{sup} , they reduce to the analogue of the classical equations of motion and the effective action Γ reduces to the free energy $-\mathcal{W}$. In the following we will suppress the supremum index for convenience and the evaluation at the supremum is understood implicitly unless stated otherwise. Note that in the derivation of (1.7) from (1.5) the term stemming from the ϕ -dependence of J_{sub} drop out:

$$\int d^d x' \frac{\delta J_{\text{sup}}(x')}{\delta \phi(x)} \phi(x') + J_{\text{sup}}(x) - \int d^d x' \frac{\delta J_{\text{sup}}(x')}{\delta \phi(x)} \left. \frac{\delta \mathcal{W}[J]}{\delta J(x')} \right|_{J_{\text{sup}}} = J_{\text{sup}}(x) \quad (1.8)$$

At this point some comments about our notation are in order. Sometimes a different normalization is used for the Schwinger functional where

$$\ln \mathcal{Z}[J] \rightarrow \ln \mathcal{Z}[J] - \ln \mathcal{Z}_0[0]. \quad (1.9)$$

¹Our Fourier conventions are detailed in appendix 2.1.

Here \mathcal{Z}_0 is the generating functional in (1.2) with the classical action replaced by the interaction-free part of it. Such a normalization leads to an additional $\ln \mathcal{Z}_0[0]$ in (1.5). This way, $\Gamma[0]$ vanishes in the interaction-free case and thus can be interpreted as the interaction correction to the free energy. Furthermore, one finds versions of the generating functional for 1PI correlation functions, (1.5), where the interaction-free part of the classical action is added. Consequently, the corresponding two-point function becomes the irreducible self energy instead of the propagator as it is the case in our notation as we will show next.

In functional approaches to quantum field theories, the two-point function is the central quantity. Therefore we discuss it here in more detail. For this purpose and in order to obtain the Legendre transform of connected n -point correlation functions for $n \geq 2$ in general one can utilize the following Legendre transform of the functional derivatives

$$\frac{\delta}{\delta J(x)} = \int d^d x' \left(\frac{\delta^2 \Gamma}{\delta \phi(x) \delta \phi(x')} \right)^{-1} \frac{\delta}{\delta \phi(x')}, \quad \frac{\delta}{\delta \phi(x)} = \int d^d x' \left(\frac{\delta^2 \mathcal{W}}{\delta J(x) \delta J(x')} \right)^{-1} \frac{\delta}{\delta J(x')}, \quad (1.10a)$$

which reads in momentum space

$$\frac{\delta}{\delta J(p)} = \int \frac{d^d p'}{(2\pi)^d} \left(\frac{\delta^2 \Gamma}{\delta \phi(-p) \delta \phi(p')} \right)^{-1} \frac{\delta}{\delta \phi(p')}, \quad \frac{\delta}{\delta \phi(p)} = \int \frac{d^d p'}{(2\pi)^d} \left(\frac{\delta^2 \mathcal{W}}{\delta J(-p) \delta J(p')} \right)^{-1} \frac{\delta}{\delta J(p')}. \quad (1.10b)$$

However, before discussing the 1PI two-point function we start with its connected version. We know from its definition that the Schwinger functional $\mathcal{W}[J]$ and the generating functional $\mathcal{Z}[J]$ are interrelated. Taking another functional derivative of (1.6) with respect to J leads to the following relationship between the two-point function and its connected part (see also the line $n = 2$ in Table 1.1):

$$\frac{\delta^2 \mathcal{W}[J]}{\delta J(x) \delta J(y)} = \frac{1}{\mathcal{Z}} \frac{\delta^2 \mathcal{Z}[J]}{\delta J(x) \delta J(y)} - \langle \varphi(x) \rangle \langle \varphi(y) \rangle. \quad (1.11)$$

The most efficient way to store the information about our QFT are the 1PI correlation functions as explained above. Therefore, we are interested in the 1PI two-point function. The definition of the effective action (1.5) establishes its relation to the Schwinger functional. Using the Legendre transforms (1.6) and (1.10) we find the relation among the corresponding two-point functions as

$$\frac{\delta^2 \mathcal{W}}{\delta J(x) \delta J(y)} = \int d^d x' \left(\frac{\delta^2 \Gamma}{\delta \phi(x) \delta \phi(x')} \right)^{-1} \frac{\delta}{\delta \phi(x')} \phi(y) = \left(\frac{\delta^2 \Gamma}{\delta \phi(x) \delta \phi(y)} \right)^{-1}. \quad (1.12)$$

This shows that the connected two-point function, also known as the full (connected) propagator is the inverse of the 1PI two-point function. The former describes the propagation of a particle from a spacetime point x to a spacetime point y and is denoted as $G(x, y)$, see also above. As this is a very important quantity let us summarize our findings about it by writing

$$G(x, y) = \langle \varphi(x) \varphi(y) \rangle_{\text{connected}} = \frac{\delta^2 \mathcal{W}}{\delta J(x) \delta J(y)} = \frac{1}{\Gamma^{(2)}(x, y)}. \quad (1.13)$$

Here, we introduced the notation $\Gamma^{(2)}$ for the 1PI two-point function of the effective action which is generalized for the 1PI n -point function by

$$\Gamma^{(n)}(x_1, \dots, x_n) = \frac{\delta^n \Gamma}{\delta \phi(x_1) \dots \delta \phi(x_n)}. \quad (1.14)$$

This is a very convenient shortcut which is commonly used in the literature and will be used frequently throughout the rest of this work. As explained above, these 1PI n -point functions $\Gamma^{(n)}$ comprise the same

information as e.g. the ordinary n -point correlation functions or equivalently their generating functional Eq. (1.2). Note that the $\Gamma^{(n)}$ are amputated correlation functions, where amputated means that the external legs of the corresponding Feynman diagrams have no attached propagators. The Legendre transform of the three-point function provides a very neat example for this fact.

$$\begin{aligned}\Gamma^{(3)}(x_1, x_2, x_3) &= \frac{\delta}{\delta\phi(x_1)}\Gamma^{(2)}(x_2, x_3) = \int d^d y_1 \frac{1}{\mathcal{W}^{(2)}(x_1, y_1)} \frac{\delta}{\delta J(y_1)} \frac{1}{\mathcal{W}^{(2)}(x_2, x_3)} \\ &= - \int d^d y_1 \int d^d y_2 \int d^d y_3 \frac{1}{\mathcal{W}^{(2)}(x_1, y_1)} \frac{1}{\mathcal{W}^{(2)}(x_2, y_2)} \mathcal{W}^{(3)}(y_1, y_2, y_3) \frac{1}{\mathcal{W}^{(2)}(x_3, y_3)}.\end{aligned}\quad (1.15)$$

In order to get a hand on the aforementioned information stored in the effective action Γ one can derive an explicit equation by using (1.5), (1.3) and (1.2). It reads

$$e^{-\Gamma[\phi]} = \int [d\varphi]_{\text{ren}} \exp \left\{ -S[\varphi + \phi] + \int d^d x \varphi(x) \frac{\delta\Gamma[\phi]}{\delta\phi(x)} \right\}. \quad (1.16)$$

Eq. (1.16) provides a very convenient closed form for the effective action in terms of a functional integro-differential equation. In particular for non-perturbative problems it is hard to solve and in most cases one has to resort to numerics, either in terms of a lattice representation of (1.16) or by functional continuum methods such as functional renormalisation group equations, Dyson-Schwinger equations or nPI methods, in short functional approaches.

<Here we want to illustrate its applicability with deriving the one-loop effective action. To that end we expand in (1.16) the classical action $S[\varphi + \phi]$ in powers of the fluctuation field φ ,

$$\begin{aligned}e^{-\Gamma[\phi]} &= \int [d\varphi]_{\text{ren}} \exp \left\{ -S[\phi] - \int d^d x \left(\frac{\delta S}{\delta\varphi} - \frac{\delta\Gamma}{\delta\phi} \right)_{\varphi=\phi} \right. \\ &\quad \left. - \frac{1}{2} \int d^d x_1 \int d^d x_2 S^{(2)}(x_1, x_2) \Big|_{\varphi=\phi} \varphi(x_1)\varphi(x_2) + \dots \right\}.\end{aligned}\quad (1.17)$$

The first term in the exponent is independent of the quantum field φ and can be pulled in front of the path integral. The second term gives higher order quantum corrections since $\Gamma[\phi] = S[\phi] +$ quantum corrections. Restoring the \hbar dependence would reveal this in an expansion in powers of \hbar . Neglecting the higher terms indicated by the ellipses we are left with a Gaussian integral which can be solved to find the well known 1-loop result

$$\Gamma^{1\text{-loop}}[\phi] = S[\phi] + \frac{1}{2} \text{Tr} \ln S^{(2)}[\phi]. \quad (1.18)$$

In the remainder of the lecture we discuss functional approaches to non-perturbative quantum field theories. In the following section we very briefly discuss Dyson-Schwinger Equations as they constitute the quantum equations of motion. The largest part of these notes however will deal with the functional renormalization group as another possible way to find the effective action. This method will be introduced after a short recapitulation of renormalisation in section 1.3.

1.2 Dyson–Schwinger Equations

We have discussed that the full information about the QFT under consideration is stored within its correlation functions. It is left to access this information in a practical way. Within this section we will discuss one of the possible master equations for the effective action $\Gamma[\phi]$, the Dyson–Schwinger Equations (DSEs). They provide an explicit diagrammatic form of the quantum equations of motion in the presence of a general current, (1.7). The section 1.4 is then devoted to the functional renormalization group equation, a method to derive the effective action. However, before discussing the latter, which is the main topic of these notes, we will first concentrate on the explicit derivation of the DSEs within this section.

The Dyson-Schwinger equation is nothing but the symmetry identity of the path integral that entails the translation invariance of the path integral measure $[d\varphi]_{\text{ren}}$ under $\varphi(x) \rightarrow \varphi(x) + f(x)$, and hence the translation invariance of the correlation functions. An infinitesimal shift is generated by the functional derivative with respect to $\varphi(x)$. In the path integral it leads us to

$$\frac{1}{Z[J]} \int [d\varphi]_{\text{ren}} \frac{\delta}{\delta\varphi(x)} \left[\exp \left(-S[\varphi] + \int d^d x' J(x') \varphi(x') \right) \right] = 0, \quad (1.19)$$

the functional integral of a total derivative vanishes. Performing the functional derivative on the right hand side of this equation leads to

$$J(x) = \left\langle \frac{\delta S[\varphi]}{\delta\varphi(x)} \right\rangle_J. \quad (1.20)$$

With (1.7) this leads us to the simple relation

$$\frac{\delta\Gamma[\phi]}{\delta\phi(x)} = \left\langle \frac{\delta S[\varphi]}{\delta\varphi(x)} \right\rangle_{J_{\text{sub}}}, \quad (1.21)$$

the expectation value of the classical EoM is equivalent to its quantum version. Still, for a closed form we have to rewrite the right hand side of (1.20) in terms of Γ .

Depending on the explicit form of the classical action $S[\varphi]$, the expectation value of its functional derivative with respect to the quantum field φ depends on various correlation functions. These can be rewritten as follows:

$$\begin{aligned} \langle \varphi(x_1) \dots \varphi(x_n) \rangle_J &= \frac{1}{Z[J]} \int [d\varphi]_{\text{ren}} \varphi(x_1) \dots \varphi(x_n) \exp \left(-S + \int d^d x' J(x') \varphi(x') \right) \\ &= \left(\frac{\delta}{\delta J(x_1)} + \langle \varphi(x_1) \rangle \right) \langle \varphi(x_2) \dots \varphi(x_n) \rangle_J \\ &= \left(\frac{\delta}{\delta J(x_1)} + \langle \varphi(x_1) \rangle \right) \dots \left(\frac{\delta}{\delta J(x_n)} + \langle \varphi(x_n) \rangle \right). \end{aligned} \quad (1.22)$$

Here we used the step from the first to the second line recursively to find the result in the last line. The expectation value of the quantum field is just the mean field and thus (1.10) results in the following Legendre transform of this expression:

$$\langle \varphi(x_1) \dots \varphi(x_n) \rangle_J = \prod_{i=1}^n \left(\int d^d x'_i G(x_i, x'_i) \frac{\delta}{\delta\phi(x'_i)} + \phi(x_i) \right), \quad (1.23)$$

with $G(x, y)$ being the inverse of $\Gamma^{(2)}(x, y)$. This can be used to rewrite (1.20) in terms of the classical action, the effective action and the classical field. Inserting the result into the quantum EoM (1.7) and introducing the shorthand $G \cdot \frac{\delta}{\delta\phi}$ for the operator product on the right hand side of (1.23) we finally find a closed expression of the quantum EoM, which reads

$$\frac{\delta\Gamma}{\delta\phi(x)} = \frac{\delta S}{\delta\varphi(x)} \left[\varphi = G \cdot \frac{\delta}{\delta\phi} + \phi \right]. \quad (1.24)$$

Eq. (1.24) is the master DSE for the 1PI correlation functions in its final form. The DSE for any 1PI n -point correlation function can be obtained via the $(n - 1)$ st functional derivative with respect to the mean field ϕ . Note that equivalent master DSEs can be derived for the correlation functions (1.1) and the connected correlation functions obtained from the Schwinger functional. Here we will discuss only the 1PI correlation functions and therefore will skip the prefix 1PI in the following.

Let us illustrate this procedure at the example of a scalar theory with a classical action $S[\varphi]$ including a φ^4 interaction given by

$$S[\varphi] = \int d^d x \left[\frac{1}{2} \partial^\mu \varphi(x) \partial_\mu \varphi(x) + \frac{m^2}{2} \varphi(x)^2 + \frac{\lambda}{4!} \varphi(x)^4 \right]. \quad (1.25)$$

Within this exemplary theory we can illustrate the general procedure, however in more realistic theories the inclusion of fermions or gauge fields introduces some subtleties, which we will not discuss here. The interested reader might find further details in DSE-reviews, e.g. [1, 2, 3, 4, 4].

Nevertheless, if we restrict ourselves for illustrative purposes to the simple scalar example (1.25) the right hand side of the master DSE (1.24) reads

$$\frac{\delta S}{\delta\varphi(x)} \left[\varphi = G \cdot \frac{\delta}{\delta\phi} + \phi \right] = \underbrace{-\partial_\mu^2 \phi(x) + m^2 \phi(x) + \frac{\lambda}{3!} \phi(x)^3}_{\frac{\delta S}{\delta\varphi(x)}[\varphi=\phi]} + \frac{\lambda}{3!} \left[\left(G \cdot \frac{\delta}{\delta\phi} + \phi \right)^3 - \phi^3 \right]. \quad (1.26)$$

The last term is rewritten as follows:

$$\begin{aligned} \left(G \cdot \frac{\delta}{\delta\phi} + \phi \right)^3 - \phi^3 &= \left(G \cdot \frac{\delta}{\delta\phi} + \phi \right)^2 \phi - \phi^3 \\ &= \left(G \cdot \frac{\delta}{\delta\phi} \right) \left(G \cdot \frac{\delta}{\delta\phi} \right) \phi + G \cdot \frac{\delta}{\delta\phi} \phi^2 + \phi G \cdot \frac{\delta}{\delta\phi} \phi \\ &= \left(G \cdot \frac{\delta}{\delta\phi} \right) G + 3G \cdot \phi \\ &= -G \cdot \left(G \cdot \Gamma^{(3)} \cdot G \right) + 3G \cdot \phi, \end{aligned} \quad (1.27)$$

where we have used in the last line that

$$\frac{\delta G}{\delta\phi} = \frac{\delta}{\delta\phi} \frac{1}{\Gamma^{(2)}} = -\frac{1}{\Gamma^{(2)}} \Gamma^{(3)} \frac{1}{\Gamma^{(2)}}. \quad (1.28)$$

Therefore, the final closed form of the master DSE for the effective action for the φ^4 theory is given by

$$\frac{\delta\Gamma[\phi]}{\delta\phi} = \frac{\delta S[\phi]}{\delta\phi} + \frac{\lambda}{2} G \cdot \phi - \frac{\lambda}{3!} G^3 \cdot \Gamma^{(3)} \quad (1.29)$$

where in the last term, all G couple to both, $\Gamma^{(3)}$ and λ . The structure of the equation is apparent in its diagrammatic representation. In Fig. 1.1(a) and Fig. 1.1(b) a transcription of the propagator and a general n -point vertex into the diagrammatic language is given. The pictorial master DSE is then given in the upper panel of Fig. 1.2.

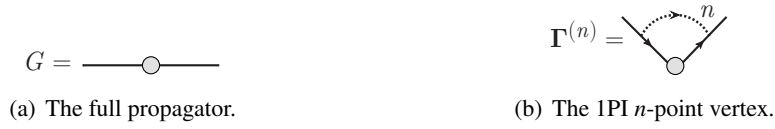


Figure 1.1: Diagrammatic representation of propagator and vertices.

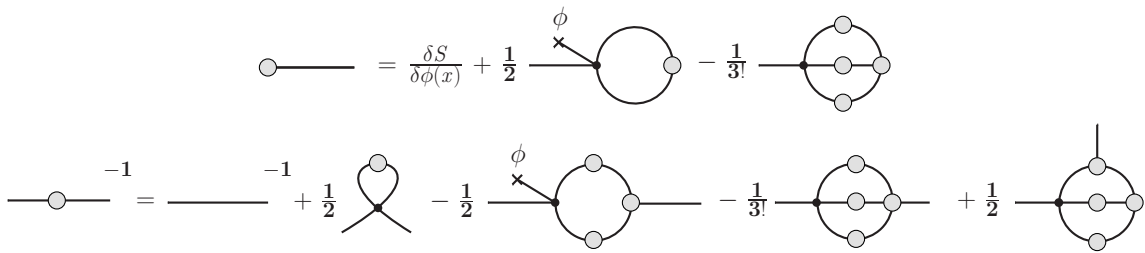


Figure 1.2: Upper panel: The graphical representation of the master Dyson-Schwinger equation.
Lower panel: The Dyson-Schwinger equation for the full inverse propagator.
The cross denotes the coupling to the non-trivial background $\phi(x)$ and the grey circles indicate full quantities.

As already mentioned, the DSEs for the general n -point functions follow from further derivatives with respect to the classical field $\phi(x)$ in (1.29). As the simplest example let us consider the scalar propagator. Its DSE, the gap equation, can be obtained from the master DSE, (1.24), by one derivative with respect to ϕ , for the diagrammatic representation see the lower panel of Fig. 1.2.

The next step would be to solve (1.29) for a generic n -point function. However, a closer look at the diagrams in Fig. 1.2 shows that for the solution of the n -point function we need to know at least the $(n + 2)$ -point function. Consequently, we are dealing with an infinite tower of coupled equations that are not always analytically solvable. Therefore, the equations have to be truncated in a physically reasonable way, i.e. with paying attention to e.g. gauge invariance, multiplicative renormalizability etc. One common technique to truncate the set of coupled equations would be by employing a specially designed vertex ansatz. For further details we refer the interested reader to DSE-reviews, e.g. [1, 2, 3, 4, 5]. Applications in QCD range from hadron resonances to the phase structure of QCD, for its relation to the functional RG see [6].

We want to close this section with a simple application as well as a comment on general functional identities derived from translation invariance. A simple as well as illuminating application of the DSE is the embedding or emergence of perturbation theory in the DSE. To that end we reproduce the one-loop effective action (1.18) we have obtained directly from the path integral representation of Γ in (1.16) within a saddle point expansion.

The one-loop effective action is obtained from (1.29) by using classical propagators $G_{\text{cl}} = 1/S^{(2)}$ and vertices on the right hand side and dropping the two-loop term. Using also $S^{(3)}[\phi] = \lambda\phi$ we are led to

the simple equation

$$\frac{\delta\Gamma[\phi]}{\delta\phi} = \frac{\delta S[\phi]}{\delta\phi} + \frac{1}{2}\text{Tr} S^{(3)}[\phi] \frac{1}{S^2[\phi]} = \frac{\delta}{\delta\phi} \left(S[\phi] + \frac{1}{2}\text{Tr} \ln S^{(2)}[\phi] \right). \quad (1.30)$$

This is nothing but the field-derivative of (1.18). Iterating this procedure leads to the higher loop diagrams including the correct combinatorial factors. It is a very simple recursive structure that elucidates part of the power of functional relations. Eq. (1.30) also highlights the fact, that the DSE does not carry the information about the field-independent part of the effective action. In the vacuum this is an irrelevant total normalisation, while at finite temperature and density it carries the thermodynamics of the theory. However, the vertices and propagators are then typically used in 2PI or 3PI resummation formulae for the thermodynamics, leading to e.g. the pressure from a combined DSE/nPI approach. This is but one example of the interesting possibility to utilise combinations of functional approaches. Here it is simply utilising results obtained in one functional approach as input in another, but it is far more general.

We close the chapter on DSEs with a remark on generalised DSEs that include also symmetry identities such as the Ward identities and Slavnov-Taylor identities that encode gauge invariance of gauge theories in a gauge-fixed setup: Eq. (1.19) can be generalised to

$$\frac{1}{\mathcal{Z}[J]} \int [d\varphi]_{\text{ren}} \frac{\delta}{\delta\varphi(x)} \left[\Psi[\varphi] \exp \left(-S[\varphi] + \int d^d x' J(x') \varphi(x') \right) \right] = 0. \quad (1.31)$$

The functional $\Psi[\varphi]$ in (1.31) can be used to derive DSEs for composite operators or for symmetry transformations. In the latter case Ψ has to be chosen such that $\delta/\delta\varphi(x)\Psi[\varphi]$ generates the symmetry operations. For example, $\Psi = 1$ provides the standard DSE, note that the $\delta/\delta\varphi(x)$ acts also to the right of Ψ . In gauge theories with gauge field A_μ and covariant derivative D_μ the choice $\Psi = D_\mu$ with $\delta/\delta A_\mu(x) D_\mu$ generates gauge transformations on the gauge field. For more details and in particular the derivation of explicit symmetry identities see e.g. [6].

1.3 Renormalization

So far we have only discussed different formal representations of the effective action. The applications, i.e. the perturbative evaluation of the effective action (at the 1-loop level) in (1.18) and (1.30), and the DSEs for the 1PI n -point functions via functional derivatives of (1.24) are by themselves simple formal expressions but suffer from standard loop divergences. that originate in the momentum integrations contained in the trace of (1.18), and the loop structure visualized in Fig. 1.2.

In this section we recapitulate how to such divergences are cured via the standard field theoretical regularisation and renormalisation procedure. For this purpose we utilize again the simple scalar theory and discuss the perturbative renormalization as well as the Wilsonian renormalisation. The latter one is tightly linked to the more general functional renormalization group equations discussed in section 1.4.

This section is included for the benefit of the reader as a very brief reminder of standard textbook renormalisation theory. It is formulated in a way that is amiable to later functional renormalisation group applications. The RG-experienced reader may just skip this part, or go along with the quote sometimes attributed to Enrico Fermi: 'Never underestimate the joy people derive from hearing/reading something they already know.'

1.3.1 Perturbative Renormalization

Here we consider the massless scalar φ^4 theory whose classical action is the massless limit of (1.25). In momentum space it reads

$$S[\varphi] = \int \frac{d^d p}{(2\pi)^d} \frac{p^2}{2} \varphi(p) \varphi(-p) + \frac{\lambda}{4!} \int \frac{d^d p_1}{(2\pi)^d} \int \frac{d^d p_2}{(2\pi)^d} \int \frac{d^d p_3}{(2\pi)^d} \varphi(p_1) \varphi(p_2) \varphi(p_3) \varphi(-p_1 - p_2 - p_3). \quad (1.32)$$

In the following we will stick to the 1-loop approximation and therefore omit the superscript "1-loop" as it appears in (1.18) in order to lighten the notation. With this we find

$$\Gamma[\phi] = S[\phi] + \frac{1}{2} \int \frac{d^d q}{(2\pi)^d} \ln [S^{(2)}(q, q)],$$

$$S^{(2)}(p, q) = p^2 (2\pi)^d \delta^d(p - q) + \frac{\lambda}{2} \int \frac{d^d p_1}{(2\pi)^d} \phi(p_1) \phi(q - p - p_1). \quad (1.33)$$

As discussed in the previous section, the knowledge about all n -point functions is as good as the one for the effective action. The two-point function is given by

$$\frac{\delta^2 \Gamma}{\delta \phi(p_1) \delta \phi(-p_2)} = \frac{\delta^2 S}{\delta \phi(p_1) \delta \phi(-p_2)} + \frac{\lambda}{2} (2\pi)^d \delta^d(p_1 - p_2) \int \frac{d^d q}{(2\pi)^d} \frac{1}{q^2}. \quad (1.34)$$

Here p_1 and p_2 are the ingoing and outgoing momenta and the $(2\pi)^d \delta^d(p_1 - p_2)$ is nothing but the momentum conservation. The integral is quadratically divergent in four dimensions which comes as a surprise since the 1PI two-point function should be finite as it can be related to observables. For the time being we take care of this divergence by introducing a finite momentum cutoff Λ ,

$$\int \frac{d^d q}{(2\pi)^d} \frac{1}{q^2} \rightarrow 2v_d \int_0^{\Lambda^2} dq^2 (q^2)^{(d-4)/2} \quad \text{with} \quad v_d = 2^{d+1} \pi^{d/2} \Gamma(d/2), \quad (1.35)$$

with the Gamma function $\Gamma(d/2)$. We leave this regularized version for the moment as it is and consider next the 4-point function, as the 3-point function vanishes at $\phi = 0$,

$$\frac{\delta^4 \Gamma}{\delta\phi(p_1)\delta\phi(p_2)\delta\phi(p_3)\delta\phi(p_4)} = S^{(4)} - \frac{\lambda^2}{2}(2\pi)^d \delta^d \left(\sum_i p_i \right) \int \frac{d^d q}{(2\pi)^d} \left\{ \frac{1}{p^2} \left[\frac{1}{(q+p_1+p_2)^2} + \frac{1}{(q+p_1+p_3)^2} + \frac{1}{(q+p_1+p_4)^2} \right] \right\}. \quad (1.36)$$

Here $s = (p_1 + p_2)^2$, $t = (p_1 + p_3)^2$ and $u = (p_1 + p_4)^2$ are the Mandelstam variables and for the sake of simplicity we will specify $s = t = u = p^2$ in the following. With this we find

$$\Gamma^{(4)} = S^{(4)} - 3v_d \lambda^2 (2\pi)^d \delta^d \left(\sum_i p_i \right) \int_0^{\Lambda^2} dp^2 \frac{q^{2\frac{d-4}{2}}}{(q+p)^2} \quad (1.37)$$

which is logarithmically divergent in four dimensions. Considering higher n -point functions we find them to be (UV-) finite due to the increasing numbers of propagators.

In summary, the first explicit evaluation we did even for the simple massless scalar theory in $d = 4$ reveals divergences in the n -point functions for $n = 2, 4$. These, however, are related to observables and thus should stay finite. On the other hand we find the coupling constant λ in our divergent expressions which is a parameter of our classical i.e. microscopic theory and therefore not observable. In the following we will renormalize our theory by shifting the divergences of our n -point functions into the coupling constant λ which we will call bare coupling in the following. In order to do so we introduce renormalized quantities marked with an index R via

$$\phi = \sqrt{Z_\phi} \phi_R, \quad \lambda = \frac{Z_\lambda}{Z_\phi^2} \lambda_R. \quad (1.38)$$

The aim is to keep the renormalized coupling, λ_R , finite and expand in powers of this instead of the bare coupling λ . For this purpose a reorganization of the classical action is in order. With (1.32) and (1.38) we can rewrite S as follows:

$$\begin{aligned} S[\phi] &= S_R[\phi_R] + \delta S[\phi_R], \\ S_R[\phi_R] &= \int \frac{d^d p}{(2\pi)^d} \frac{p^2}{2} \phi_R(p) \phi_R(-p) \\ &\quad + \frac{\lambda_R}{4!} \int \frac{d^d p_1}{(2\pi)^d} \int \frac{d^d p_2}{(2\pi)^d} \int \frac{d^d p_3}{(2\pi)^d} \phi_R(p_1) \phi_R(p_2) \phi_R(p_3) \phi_R(-p_1 - p_2 - p_3), \\ \delta S[\phi_R] &= \delta Z_\phi \int \frac{d^d p}{(2\pi)^d} \frac{p^2}{2} \phi_R(p) \phi_R(-p) \\ &\quad + \frac{\lambda_R}{4!} \delta Z_\lambda \int \frac{d^d p_1}{(2\pi)^d} \int \frac{d^d p_2}{(2\pi)^d} \int \frac{d^d p_3}{(2\pi)^d} \phi_R(p_1) \phi_R(p_2) \phi_R(p_3) \phi_R(-p_1 - p_2 - p_3), \end{aligned} \quad (1.39)$$

with $\delta Z_\phi = Z_\phi - 1$ and $\delta Z_\lambda = Z_\lambda - 1$. Next we assume that δS is of higher order in λ_R than S_R which we will verify with hindsight. With this assumption we can perform the 1-loop analysis with S_R only as δS gives a higher order contribution. Thus we have at 1-loop order

$$\Gamma_R[\phi_R] = \Gamma[\phi] = S[\phi] + \frac{1}{2} \text{Tr} \ln S^{(2)} = S_R[\phi_R] + \delta S[\phi_R] + \frac{1}{2} \text{Tr} \ln S_R^{(2)}. \quad (1.40)$$

The renormalised $\text{Tr} \ln$ term will result in the expressions (1.34) and (1.37) with λ replaced by λ_R . Therefore, the divergences persist. However, this time we can use the counterterms, δS , to subtract these divergences and obtain a finite result. Explicitly we find for $s = t = u = p^2$,

$$\Gamma_R^{(4)} = Z_\lambda \lambda_R - 3v_d \lambda_R^2 \int_0^{\Lambda^2} d^d q^2 \frac{(q^2)^{(d-2)/2}}{p^2(q+p)^2} = Z_\lambda \lambda_R - 3v_d \lambda_R^2 \int_0^{\Lambda^2} d^d q^2 \int_0^1 dx \frac{q^{2\frac{d-2}{2}}}{[q^2 + x(1-x)p^2]^2} \quad (1.41)$$

where we used the Feynman parameter x to rewrite the result. Typically we will assign q for loop momenta and p for external momenta. Now Z_λ is at our disposal and we can choose it as we like, as long as it cancels the divergence in the loop integral. In four dimensions we write

$$Z_\lambda = 1 + \lambda_R \left[\frac{3\lambda_R}{32\pi^2} \ln(\Lambda^2/p^2) + c_\lambda^{(1)} \right] + \mathcal{O}(\lambda_R^2) \quad (1.42)$$

where the 1 in front assures that the counterterm δS is of higher order in λ_R according to our assumption above. Furthermore, $c_\lambda^{(1)}$ is at our disposal and we neglected higher orders in λ_R . With this we find that the 4-point function (1.41) is finite.

The freedom of choosing $c_\lambda^{(1)}$ is called renormalization scheme dependence and here we opt for the so-called momentum subtraction scheme, i.e. we fix $c_\lambda^{(1)}$ by asking for the following renormalization condition:

$$\Gamma_R^{(4)}(p^2 = \mu^2) = \lambda_R. \quad (1.43)$$

The new energy scale μ is called renormalization scale and we find that the infinities of our n -point functions have been traded for a dependence on the new scale μ . The dependence on this new scale is described by differential equations. To find such an equation we start with the first equality in (1.40) to find

$$\begin{aligned} \Gamma^{(n)}(Q_i, \lambda, \Lambda) &= Z_\phi^{-n/2} \Gamma_R^{(n)}(Q_i, \lambda_R, \mu) \\ \Rightarrow 0 &= \mu \frac{d}{d\mu} \Gamma^{(n)}(Q_i, \lambda, \Lambda) = \left[\mu \frac{\partial}{\partial \mu} + \beta_\lambda(\lambda_R) \frac{\partial}{\partial \lambda_R} - \frac{n}{2} \eta(\lambda_R) \right] \Gamma_R^{(n)}(Q_i, \lambda_R, \mu). \end{aligned} \quad (1.44)$$

Here we introduced the beta function, β_λ , and the anomalous dimension, η as

$$\beta_\lambda(\lambda_R) = \mu \frac{d}{d\mu} \lambda_R, \quad \eta(\lambda_R) = \frac{\mu}{Z_\phi} \frac{dZ_\phi}{d\mu} \quad (1.45)$$

with the derivatives evaluated at fixed bare coupling λ . For the renormalization condition (1.43) we find

$$\beta_\lambda = \mu \frac{d}{d\mu} \left(\frac{Z_\phi^2}{Z_\lambda} \lambda \right) = 2\eta \lambda_R - \frac{\lambda_R}{Z_\lambda} \mu \frac{d}{d\mu} Z_\lambda = 2\eta \lambda_R + \frac{3\lambda_R^2}{16\pi^2} + \mathcal{O}(\lambda_R^3). \quad (1.46)$$

The contribution with the anomalous dimension comes from the field renormalization, (1.38), and the loop correction leads to the second term. A similar evaluation for the momentum-square part of the 2-point function would reveal $Z_\phi = 1$ and therefore $\eta = 0$ at 1-loop order.

To get an idea of how to interpret the renormalization scale μ which was introduced in a kind of arbitrary way via the renormalization condition we analyze the theory under a change of momentum scale. However, before rescaling the theory let us summarize the dimensionality of some quantities in order to fix our notation. In the following we will use the square bracket to define the dimension in powers of momenta, i.e.

$$\begin{aligned} [p] &= 1, & [x] &= -1, & [\phi(x)] &= d_\phi = \frac{d-2}{2}, & [\phi(p)] &= d_\phi - d, & [\Gamma] &= 0, \\ [\delta^d(p)] &= -d, & \left[\frac{\delta}{\delta\phi(p)} \right] &= -d_\phi, & \left[\frac{\delta}{\delta\phi(x)} \right] &= d - d_\phi. \end{aligned} \quad (1.47)$$

The corresponding scaling behavior of the field thus reads $\phi(tx) = t^{-d_\phi}\phi(x)$ and $\phi(tp) = t^{d_\phi-d}\phi(p)$. At this point a comment is in order regarding our sloppy notation of incorporating the momentum conservation into the n -point function. The dimensional analysis goes as follows:

$$\begin{aligned} \Gamma^{(n)}(Q_1, \dots, Q_n) &= \Gamma^{(n)}(Q_1, \dots, Q_{n-1}) (2\pi)^d \delta^d(\sum_i Q_i) \\ [\Gamma^{(n)}(Q_1, \dots, Q_n)] &= -n \frac{d-2}{2} \quad \Rightarrow \quad [\Gamma^{(n)}(Q_1, \dots, Q_{n-1})] = d - n \frac{d-2}{2}. \end{aligned} \quad (1.48)$$

This then clarifies any possible confusion about the dimensional analysis of (1.43) which reads

$$[\Gamma_{\text{R}}^{(4)}(Q^2 = \mu^2)] = d - 2d + 4 = 4 - d = [\lambda_{\text{R}}] \quad (1.49)$$

and gives a dimensionless coupling in four dimensions.

With this input we can now discuss the 4-point function in context of a momentum rescaling. The process described by a 4-point function is a $2 \rightarrow 2$ scattering process and the external momenta Q_i define the relevant scale for this process. Now consider the same process at a different scale which might be obtained via $Q'_i = t Q_i$. Next, relate this to the same process at the external momenta Q_i with a suitable rescaling of the theory, i.e. $Q'_i \rightarrow Q'_i/t, \mu \rightarrow \mu/t$ and $\lambda_{\text{R}} \rightarrow \lambda_{\text{R}} t^{-[\lambda]}$. We find

$$\Gamma_{\text{R}}^{(4)}(Q'_1, Q'_2, Q'_3, \lambda_{\text{R}}, \mu) = t^{4-d} \Gamma_{\text{R}}^{(4)}\left(Q_1, Q_2, Q_3, \frac{\lambda_{\text{R}}}{t^{[\lambda]}}, \frac{\mu}{t}\right) \quad (1.50)$$

which finally can be used to study the change of $\Gamma_{\text{R}}^{(4)}$ under a rescaling of the momentum to obtain

$$\begin{aligned} t \frac{d}{dt} \Gamma_{\text{R}}^{(4)}(Q'_1, Q'_2, Q'_3, \lambda_{\text{R}}, \mu) &= \left[(4-d) - [\lambda] \lambda_{\text{R}} \frac{\partial}{\partial \lambda_{\text{R}}} - \mu \frac{\partial}{\partial \mu} \right] \Gamma_{\text{R}}^{(4)}(Q'_1, Q'_2, Q'_3, \lambda_{\text{R}}, \mu) \\ &= \left[(\beta_\lambda - [\lambda] \lambda_{\text{R}}) \frac{\partial}{\partial \lambda_{\text{R}}} + 4 - d - 2\eta \right] \Gamma_{\text{R}}^{(4)}(Q'_1, Q'_2, Q'_3, \lambda_{\text{R}}, \mu) \end{aligned} \quad (1.51)$$

where we used (1.44) to replace the μ dependence.

After all this dimensional analysis we finally traded the μ dependence described by (1.44) for a t dependence described by (1.51). The latter one has a clear interpretation in terms of rescaling the external momenta. To finalize the replacement we now search for a replacement of the μ dependence of the renormalized coupling given in terms of the beta function by a suitable t dependence. In other words we aim at $\lambda_{\text{R}}(t)$ and $f(t)$ such that this t dependence compensates for the change of $\Gamma_{\text{R}}^{(4)}$ due to the rescaling, i.e.

$$\Gamma_{\text{R}}^{(4)}(Q'_1, Q'_2, Q'_3, \lambda_{\text{R}}, \mu) = f(t) \Gamma_{\text{R}}^{(4)}(Q_1, Q_2, Q_3, \lambda_{\text{R}}(t), \mu). \quad (1.52)$$

Inserting this into (1.51) and comparing the left and the right hand side one finds the t dependence of λ_{R} and f as

$$t \frac{d\lambda_{\text{R}}}{dt} = -[\lambda] \lambda_{\text{R}} + \beta_\lambda = -[\lambda] \lambda_{\text{R}} + 2\eta \lambda_{\text{R}} + \frac{3\lambda_{\text{R}}^2}{16\pi^2}, \quad \frac{t}{f(t)} \frac{df(t)}{dt} = 4 - d - 2\eta. \quad (1.53)$$

Phrasing this result in words, we have shown that a change of the relevant scale generated a change of the coupling in three steps: First, one obtains a change due to quantum corrections, encoded in the last term of the flow equation for λ_{R} . The second contribution stems from the field renormalization encoded in η and finally one obtains a dimensional rescaling according to the dimension of the coupling, $[\lambda] = 4 - d$. Notably, introducing the dimensionless coupling constant by multiplying with a suitable power of the renormalization scale μ , $\lambda_{\text{R}} \mu^{-[\lambda_{\text{R}}]}$, and evaluating its logarithmic scale derivative one obtains the same form:

$$\mu \frac{d}{d\mu} \frac{\lambda_{\text{R}}}{\mu^{4-d}} = (d-4) \lambda_{\text{R}} + \beta_\lambda. \quad (1.54)$$

We will come back to this point in section ??.

Before we redo the renormalization procedure starting from a different viewpoint, namely the Wilsonian one, let us summarize what we did in this subsection. We started with evaluating the effective action in a 1-loop approximation. To be precise we evaluated the two- and four-point function. While doing so we realized that in general the quantum corrections lead to divergences. Since the 1PI n -point functions are related to observables they should stay finite. Thus we "shifted" the divergence into the bare coupling constant λ which describes the microscopic physics but might be the wrong parameter for macroscopic physics. This shift was done by introducing a renormalized coupling constant λ_R in (1.38) where we included quantum fluctuations in Z_λ and the effect of field renormalization in Z_ϕ . The renormalized quantities came with a renormalization condition, introducing a new scale μ . The scale dependence $\lambda_R(\mu)$ was finally traded for a t dependence describing a rescaling of the theory. This means that we have to adapt the coupling in our theory while changing the relevant scale of the process to be described. In short, we did three steps: integrating out the quantum fluctuations (within a 1-loop approximation), renormalizing the fields and rescaling the theory.

1.3.2 Wilsonian Renormalization

Recapitulating the previous subsection one might be uncomfortable with the fact that one subtracts divergences to obtain a finite result. This can be circumvented with the Wilsonian viewpoint on renormalization which will be described in the following. Furthermore, this viewpoint lays the ground for the functional renormalization group method introduced in the next section. We start with the generating functional (1.2),

$$\mathcal{Z}_\Lambda[J] = \frac{1}{\mathcal{N}} \int_\Lambda [d\varphi] \exp \left\{ -S_\Lambda[\varphi] + \int d^d x \varphi(x) J(x) \right\}, \quad (1.55)$$

where the index Λ at \mathcal{Z} and the integral indicates an integration over modes $\varphi(p)$ with $p^2 < \Lambda^2$.² The classical action S receives an index Λ as well for reasons that will become clear soon. The restriction of momenta is ensuring the finiteness of the results as we have seen in the previous subsection. For well defined theories this cutoff can be removed by sending $\Lambda \rightarrow \infty$ at the end.

Since the divergences of the previous subsection have been related to an integration over all momenta we will perform this momentum integration step by step, i.e. momentum shell by momentum shell. For this purpose we introduce a new cutoff $\Lambda' < \Lambda$ and distinguish between soft and hard modes which we denote by $\tilde{\varphi}$ and $\hat{\varphi}$ respectively. They are defined as

$$\begin{aligned} \tilde{\varphi}(p) &= \varphi(p) \Theta(\Lambda' - |p|), \\ \hat{\varphi}(p) &= \varphi(p) [1 - \Theta(\Lambda' - |p|)], \end{aligned} \quad (1.56)$$

with the Heaviside function Θ . Thus, we have $\varphi = \tilde{\varphi} + \hat{\varphi}$ and can rewrite the path integral in (1.55) in terms of $\tilde{\varphi}$ and $\hat{\varphi}$ and integrate out the hard modes to find

$$\begin{aligned} \mathcal{Z}_\Lambda[J] &= \frac{1}{\mathcal{N}} \int_{\Lambda'} [d\tilde{\varphi}] \int_\Lambda [d\hat{\varphi}] \exp \left\{ -S_\Lambda[\tilde{\varphi}, \hat{\varphi}] + \int d^d x [\tilde{\varphi}(x) J(x) + \hat{\varphi}(x) J(x)] \right\} \\ &= \frac{1}{\mathcal{N}} \int_{\Lambda'} [d\tilde{\varphi}] \exp \left\{ -S_{\Lambda'}[\tilde{\varphi}] + \int d^d x \tilde{\varphi}(x) J(x) \right\}. \end{aligned} \quad (1.57)$$

²Note that at this point the reason for choosing Euclidean conventions from the very beginning reveals itself. Within Minkowski space we would have light-like momenta with large components and small absolute value. This would hinder a useful definition of $p^2 < \Lambda^2$.

$$\begin{aligned}
S_\Lambda &\sim \int d^d \mathbf{x} g_4 \varphi^4 \sim \text{X} \\
S_{\Lambda'} &\sim \int d^d \mathbf{x} [g'_4 \tilde{\varphi}^4 \sim \text{X} + \text{O} + \dots \\
&+ g'_6 \tilde{\varphi}^6 \sim \text{O} + \dots \\
&\dots] \sim \dots
\end{aligned}$$

Figure 1.3: Graphical example for the generation of new couplings in the process of integrating out quantum fluctuations of a momentum shell.

After performing this integral (which is in general everything but trivial) we are left with a functional integral over the soft modes, $\tilde{\varphi}$, with a new action $S_{\Lambda'}$ in the exponent. The latter is given via

$$\exp\{-S_{\Lambda'}[\tilde{\varphi}]\} = \int_{\Lambda} [d\hat{\varphi}] \exp\left\{-S_{\Lambda}[\tilde{\varphi}, \hat{\varphi}] + \int d^d x \hat{\varphi}(x) J(x)\right\}, \quad (1.58)$$

and thus has the structure of a Schwinger functional. It contains quantum corrections which might induce new couplings. This is depicted for the exemplary φ^4 theory in Fig. 1.3. The external legs are soft and the internal propagating particles are hard modes. In general any kind of new coupling which respects the symmetry of the underlying theory is produced. When there is a controlled expansion as e.g. in perturbation theory it might be possible to neglect these new couplings as the corresponding contributions are of higher order in the expansion. For strongly coupled systems this simplification is not valid. We will come back to this point in section 1.5.

This procedure of integrating out the quantum fluctuations of the hard modes within the momentum shell might be performed iteratively, which finally results in a complete integration of all modes. The advantage of this procedure above the one described in the previous subsection is that the couplings are modified successively which circumvents the problem of subtracting divergences to get a finite result.

Another step in the previous subsection was the rescaling which shall be performed here as well. For the sake of definiteness let us perform this rescaling at the example of the massless φ^4 theory discussed in the previous subsection. The classical action (1.32) receives quantum corrections and the new action in

the exponent can be written down and rescaled as follows,

$$\begin{aligned}
S_{\Lambda'} &= \int \frac{d^d p}{(2\pi)^d} \left[\frac{p^2}{2} (1 + \Delta Z) + \frac{\Delta m^2}{2} \right] \varphi(p) \varphi(-p) \\
&\quad + \frac{\lambda + \Delta \lambda}{4!} \int \frac{d^d p_1}{(2\pi)^d} \int \frac{d^d p_2}{(2\pi)^d} \int \frac{d^d p_3}{(2\pi)^d} \varphi(p_1) \varphi(p_2) \varphi(p_3) \varphi(-p_1 - p_2 - p_3) + \dots \\
&= \int \frac{d^d p'}{(2\pi)^d} \left[\frac{p'^2}{2} + \frac{m'^2}{2} \right] \varphi'(p') \varphi'(-p') \\
&\quad + \frac{\lambda'}{4!} \int \frac{d^d p'_1}{(2\pi)^d} \int \frac{d^d p'_2}{(2\pi)^d} \int \frac{d^d p'_3}{(2\pi)^d} \varphi'(p'_1) \varphi'(p'_2) \varphi'(p'_3) \varphi'(-p'_1 - p'_2 - p'_3) + \dots
\end{aligned} \tag{1.59}$$

Here, ΔZ , Δm^2 and $\Delta \lambda$ denote the corrections and the ellipses indicate further terms which might be produced but shall not be considered in the following. In the second equality we rescaled the momenta, fields and couplings according to their dimensions as

$$\begin{aligned}
p' &= p \frac{\Lambda}{\Lambda'}, & \varphi'(p') &= \left(\frac{\Lambda}{\Lambda'} \right)^{d_\phi - d} \sqrt{1 + \Delta Z} \varphi(p), \\
m'^2 &= \left(\frac{\Lambda}{\Lambda'} \right)^2 (1 + \Delta Z)^{-1} \Delta m^2, & \lambda' &= \left(\frac{\Lambda}{\Lambda'} \right)^{[\lambda]} \frac{\lambda + \Delta \lambda}{(1 + \Delta Z)^2}.
\end{aligned} \tag{1.60}$$

Comparing the definition of λ' with the renormalized coupling of the previous subsection (1.38) one realizes that the renormalization of the fields is included here as well (in the correction ΔZ). After integrating out the hard modes and rescaling the fields and couplings the generating functional (1.55) obtains the same form but the classical action in the exponent is replaced by a modified version (1.59). The latter is called Wilsonian effective action and is related to the Schwinger functional and connected diagrams. Thus, it should not be confused with the effective action Γ related to 1PI diagrams. An explicit evaluation of ΔZ at one-loop order shall be left as an exercise and can be done analogously to the evaluation of $\Delta \lambda$ presented in Appendix 2.2. One finds

$$\Delta Z = 0, \quad \Delta \lambda = -\frac{3}{2} \lambda^2 \int \frac{d^d \hat{p}}{(2\pi)^d} \frac{1}{(\hat{p}^2)^2}, \tag{1.61}$$

where we neglected the external momenta Q_i corresponding to the soft modes in comparison to the momenta of the hard modes, \hat{p} . This contribution to λ is reminiscent of the results obtained in the previous subsection and corresponds to the second diagram in the second line of Fig. 1.3 with momenta $\Lambda'^2 < \hat{p}^2 < \Lambda^2$ running in the loop.

Now let us finalize the comparison to the perturbative renormalization by investigating the change of the coupling more closely. We find

$$\frac{\lambda' - \lambda}{\Lambda' - \Lambda} = \frac{1}{\Lambda' - \Lambda} \left\{ \left[\left(\frac{\Lambda}{\Lambda'} \right)^{[\lambda]} - 1 \right] \lambda - \frac{3\lambda^2}{16\pi^2} \left(\frac{\Lambda}{\Lambda'} \right)^{[\lambda]} \ln \left(\frac{\Lambda}{\Lambda'} \right) \right\}. \tag{1.62}$$

In order to compare our findings to the perturbative calculation we consider a logarithmic, infinitesimal change by considering the limit $\Lambda' \rightarrow \Lambda$. For convenience, we introduce a parameter t describing the rescaling via $\Lambda' = t\Lambda$ reminiscent of the one in the previous subsection. The result reads

$$\Lambda \lim_{\Lambda' \rightarrow \Lambda} \frac{\lambda' - \lambda}{\Lambda' - \Lambda} = \lim_{t \rightarrow 1} \frac{1}{t - 1} \left\{ [t^{-[\lambda]} - 1] \lambda + \frac{3\lambda^2}{16\pi^2} t^{-[\lambda]} \ln(t) \right\} = -[\lambda] \lambda + \frac{3\lambda^2}{16\pi^2}. \tag{1.63}$$

This is exactly the running coupling obtained for perturbative renormalization in (1.53) with a dimensional part and the loop correction. Going beyond the 1-loop approximation would result in $\Delta Z \neq 0$ and thus give the last contribution due to the field renormalization.

Before we introduce the functional renormalization group as a specific implementation of the Wilsonian viewpoint on renormalization let us summarize this subsection and highlight again the relation to the perturbative renormalization in the previous subsection. We started to integrate the quantum fluctuations appearing in loops not all at once but to integrate them momentum shell by momentum shell. This allowed us to circumvent the subtraction of divergences. After such a momentum-shell integration we renormalized the fields and rescaled the theory in order to obtain a path integral with the same form as before the integration which allowed for a comparison of the action in the exponent. The integration of the hard modes not only results in a change of the existing couplings but also introduces in general all new couplings which satisfy the symmetry of the underlying theory. The combination of these three steps, integration, field renormalization and rescaling, is called a renormalization group step. Making this step infinitesimally small we can investigate the logarithmic change of couplings within a differential equation describing the running coupling. Using perturbative arguments, i.e. neglecting higher orders in the coupling, we have derived such a flow equation for the scalar theory (1.63) and obtained the result of the previous subsection (1.53). The latter as well describes the change of the couplings with the scale but was obtained with a detour to the scale μ defined at the renormalization point.

1.4 Functional Renormalization Group Equations

Within this section, the discussion will be based on the effective action $\Gamma[\phi]$ which has been explained in the previous sections to be the fundamental quantity in functional approaches. In the standard momentum setting, we initiate the theory at hand at a high momentum scale $k = \Lambda$ where the theory is well described by its microscopic degrees of freedom. Then, the microscopic action $S[\phi] = \Gamma_{k=\Lambda}[\phi]$ supposedly includes the physics at this momentum scale and the propagation of modes with momenta below this scale, $p^2 \lesssim k^2 = \Lambda^2$, is suppressed. Following the Wilsonian idea of renormalization and lowering the scale k infinitesimally, the physics of the momentum shell $p^2 \in [(\Lambda - \delta k)^2, \Lambda^2]$ is included and the theory is described by the effective average action $\Gamma_{k=\Lambda-\delta k}[\phi]$. Therefore, the effects of the quantum fluctuation in the momentum shell are encoded in the change of the microscopic action $S[\phi] = \Gamma_{k=\Lambda}[\phi]$ to the effective average action $\Gamma_k[\phi]$ at the scale $k = \Lambda - \delta k$. This procedure can be repeated iteratively to find the effective average action $\Gamma_k[\phi]$ incorporating the quantum fluctuations with momenta $k^2 < p^2 < \Lambda^2$. Integrating out all quantum fluctuations, meaning $k \rightarrow 0$, finally leaves us with the full quantum effective action $\Gamma[\phi]$. A pictorial representation of this iteration is given in Fig. 1.4. For the time being we will concentrate on the integration of quantum fluctuations and leave aside the field renormalization and the rescaling discussed in the previous section. We will come back to this in section ??.

The aforementioned infinitesimal change of $\Gamma_k[\phi]$ can be extracted from the flow $\partial_k \Gamma_k[\phi]$. As we will show in the following, the latter can be written down in a simple closed form which only involves ϕ derivatives of $\Gamma_k[\phi]$. Therefore, in an FRG setting the theory is defined by specifying the initial effective (or bare) action at a high momentum scale Λ and a flow equation, $\partial_k \Gamma_k[\phi]$. This is in one-to-one correspondence to the functional DSE setting, where the theory is defined by specifying the classical action and the DSEs for the n -point functions $\Gamma^{(n)}[\phi]$. Both functional procedures are formally equivalent to a definition of the theory via a (suitably discretized version of the) path integral.

As promised above we will now derive an explicit form for the flow equation. To start with, we write down the generating functional, modified by the introduction of a scale k , discriminating between high-momentum fluctuations ($p^2 \gtrsim k^2$) and low-momentum fluctuations ($p^2 \lesssim k^2$). As explained above, the latter shall be suppressed. Thus, we write

$$\mathcal{Z}_k[J] \cong \int [d\varphi]_{\text{ren}, p^2 \gtrsim k^2} \exp\left(-S[\varphi] + \int d^d x J(x) \varphi(x)\right). \quad (1.64)$$

However, this is just a very abstract way of implementing the Wilsonian idea. The suppression of modes with momenta $p^2 \lesssim k^2$ can be implemented explicitly by defining the scale-dependent renormalised integration measure as

$$\int [d\varphi]_{\text{ren}, p^2 \gtrsim k^2} = \int [d\varphi]_{\text{ren}} \exp(-\Delta S_k[\varphi]) \quad (1.65)$$

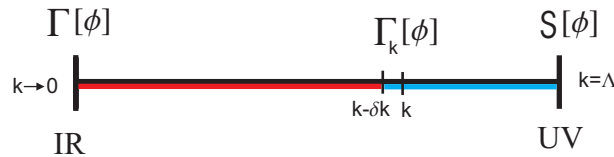


Figure 1.4: Scale-dependent effective action $\Gamma_k[\phi]$, that is the full quantum effective action for physics with momenta $p^2 \gtrsim k^2$ (blue interval). The quantum physics of momenta $p^2 \lesssim k^2$ is not included in $\Gamma_k[\phi]$, it serves as an effective classical or bare action for this regime (red interval).

where the modification to the action, ΔS_k , is given by

$$\Delta S_k[\varphi] = \frac{1}{2} \int \frac{d^d p}{(2\pi)^d} \varphi(p) R_k(p^2) \varphi(-p). \quad (1.66)$$

Here we introduced a general regulator function R_k . Since the modification is quadratic in the fields it can be interpreted as a momentum-dependent mass term with a mass proportional to the infrared scale k . Therefore, the regulator R_k can be chosen such that modes with $(p^2 \lesssim k^2)$ acquire a mass which leads to a decoupling and thus enforces a suppression of these fluctuations.

With the infrared modification of the classical action, $\Delta S_k[\varphi]$, the IR-regularised generating functional \mathcal{Z}_k is given by

$$\mathcal{Z}_k[J] = \int [d\varphi]_{\text{ren}} \exp \left[-S[\varphi] - \Delta S_k[\varphi] + \int d^d x J(x) \varphi(x) \right]. \quad (1.67)$$

Using this generalisation of the generating functional we can define the scale-dependent version of the Schwinger functional as its logarithm via $\mathcal{W}_k = \ln \mathcal{Z}_k$. Note that the Schwinger functional depending on the scale k is related to the Wilsonian effective action which we encountered in the previous section. Finally a modified Legendre transformation leads us to the scale dependent version of the effective action, the scale-dependent effective action Γ_k which we already mentioned at the beginning of this section. This modified Legendre transformation takes care of the regulator insertion ΔS_k and reads

$$\Gamma_k[\phi] = \sup_J \left\{ \int d^d x J(x) \phi(x) - \mathcal{W}_k[J] \right\} - \Delta S_k[\phi]. \quad (1.68)$$

The scale-dependent effective action has a integro-differential path integral representation similar to that of the full effective action derived in section 1.1, (1.16). It reads

$$e^{-\Gamma_k[\phi]} = \int [d\varphi]_{\text{ren}} \exp \left\{ -S[\varphi + \phi] + \int d^d x \varphi(x) \frac{\delta \Gamma_k[\phi]}{\delta \phi(x)} - \Delta S_k[\varphi] \right\}. \quad (1.69)$$

The structure is the same as in (1.16) at the end of section 1.1 with $S \rightarrow S + \Delta S_k$. This representation is very useful to discuss the limits of Γ_k in k . With the limits under control, an infinitesimal k step from $k \rightarrow k - \Delta k$, that is $\partial_k \Gamma_k$, as indicated in Fig. 1.4 resolves the full k -trajectory and hence the full effective action.

As we explained in the beginning of this section the Wilsonian idea of renormalization considers a starting point at some high energy scale Λ , where all quantum fluctuations are suppressed and the theory is described by the classical action $S[\phi]$. Since the suppression of modes within the FRG framework is obtained with the scale-dependent mass (the regulator) we have to use a diverging R_k in the limit $k \rightarrow \infty$. Since the regulator insertion ΔS_k in (1.66) is quadratic in the field it behaves as a delta function $\sim \delta[\varphi]$ in this case. This singles out the classical field configuration as the argument of the classical action under the path integral on the right hand side of (1.69). Accordingly, if the path integral is a well-defined object by itself, we would end up with the desired behaviour $\Gamma_{k \rightarrow \Lambda \rightarrow \infty}[\phi] = S[\phi]$. Strictly speaking this limit has to be defined by an appropriate block spinning procedure, and in general does not lead to the classical action, but an action which is given by all UV-relevant operators not forbidden by symmetry arguments. As this is most easily seen by using the explicit expression for $\partial_k \Gamma$, we postpone the respective discussion. On the other hand, as explained at the beginning of the section, the modification term to the action is supposed to leave us with the full quantum effective action, if we choose the momentum regulator scale $k = 0$. This can be achieved by the requirement

$$\Delta S_{k \rightarrow 0} \rightarrow 0. \quad (1.70)$$

With this limit the scale-dependent generating functional (1.67) becomes the ordinary generating functional and the same holds true for the scale-dependent version of the Schwinger functional. Since the

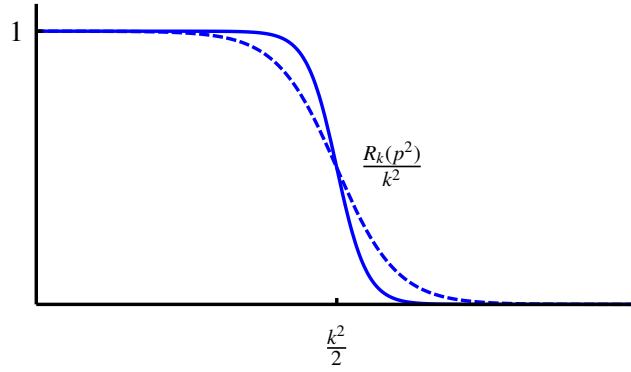


Figure 1.5: Possible choices for the regulator functions that do not modify UV modes and suppress IR modes. The depicted regulators are smeared Heaviside functions $\frac{R_k}{k^2} = 1 - \left[1 + \exp[-c(2p^2/k^2 - 1)]\right]^{-1}$ with $c = 10(20)$ for the dashed (solid) curve.

modification of the Legendre transformation (??) vanishes we finally end up with the limit $\Gamma_{k \rightarrow 0}[\phi] = \Gamma[\phi]$ which we searched for.

Let us summarise the requirements for the regulator in a more mathematical language. To that end we consider the dimensionless version of the regulator, $R_k(p)/k^2$ as well as the dimensionless momentum $y = p^2/k^2$. Then, in the absence of additional scales in the dimensionless regulator is a function of y . For the present scalar theory we have

$$R_k(p^2) = p^2 r_k(y) \quad \text{with} \quad y = \frac{p^2}{k^2}, \quad (1.71)$$

and hence $R_k/k^2(y) = y r_k(y)$. Note that r_k is a dimensionless function and typically does not depend on k , the subscript k is mere tradition and may be dropped. Moreover, we have taken the simplest choice for the prefactor, the classical dispersion p^2 . This choice is up to us and we may also take the full quantum dispersions, more details concerning these choices can be found in ???. The formulation in dimensionless momenta allows us to discuss the infrared and ultraviolet limits in a concise way.

- (i) Suppression of momentum modes with $p^2 \lesssim k^2$:

$$\lim_{y \rightarrow 0} y r_k(y) > 0, \quad (1.72a)$$

typically we have $R_k(0)/k^2 = 1$, the infrared regulator mass is k^2 , and $R_k(k^2/2)/(k^2/2) = 1/2$, the infrared suppression with the regulator gets effective at $p^2 = k^2/2$.

- (ii) Full ultraviolet quantum physics of momentum modes with $p^2 \gg k^2$:

$$\lim_{y \rightarrow \infty} y r_k(y) = 0, \quad (1.72b)$$

In Fig. 1.5 a sketch of a possible regulator is given. Note that the choice of the regulator function R_k is not unique, which is indicated in Fig. 1.5 by the dashed curve. In fact, it can be chosen at will, as long as the conditions (i) and (ii) are satisfied. Condition (i) also entails that for $k \rightarrow \infty$ all modes in the theory are suppressed and the path integral gets trivial.

In most cases we shall use regulators with $R_k(p^2 = k^2/2) = k^2/2$, see Fig. 1.5, which defines the scale at which the suppression of modes induced from the regulator grows large. Note however, that the effective cutoff scales rather is $p^2 = k^2$, as the full dispersion $p^2 + R_k(p^2)$ below this scale gets flat. This discussion is already a hint that the running cutoff scale k should not be identified directly with the physical infrared cutoff scale k_{phys} . In general one should keep in mind that k_{phys} is related but not identical with the scale k in the regulator.

Although we are free to choose a regulator, the physics of a system does not depend on this choice since it is extracted at $k = 0$. For the benefit of the reader we quote some frequently used regulators,

$$\begin{aligned}
\text{Litim cutoff: } r_k(y) &= \left(\frac{1}{y} - 1\right) \Theta(1 - y), \\
\text{exponential cutoff: } r_k(y) &= \frac{1}{\exp(cy^b) - 1}, \\
\text{sharp cutoff: } r_k(y) &= \frac{1}{\Theta(y - 1)} - 1, \\
\text{Callan-Symanzik cutoff: } r_k(y) &= \frac{1}{y}, \tag{1.73}
\end{aligned}$$

with $\Theta(x)$ being the Heaviside step function and c, b being parameters to be chosen by hand. Each regulator has its advantages and its drawbacks. The Litim regulator will be discussed in more detail in section ?? and we should mention at least that the exponential regulator is very well suited for numerical implementations. The sharp cutoff implements explicitly the Wilsonian idea of momentum shell-wise integration. The soft modes ($y < 1$) become infinitely heavy and decouple while the hard modes ($y > 1$) do not receive any modifications and are integrated out. Finally the Callan-Symanzik cutoff is an additional mass $R_k(p^2) = k^2$ and leads to the Callan-Symanzik equation [7, 8, 9].

Note also that the Callan-Symanzik equation is formally different from the other regulator choices, as it describes the change of a fundamental relevant operator in the theory. This is reflected by the fact that it does not satisfy the condition (ii), (1.72b). Accordingly, a change in k then changes the theory and its renormalisation as it changes the mass. In turn, a momentum-local modification with (1.72b) integrates out degrees of freedom in a given theory, the UV renormalisation is not affected by this. Interestingly, the more general modifications have been briefly discussed in [8, 9], which anyway gives an impressively modern account of functional flow equations. Despite this deficiencies of the Callan-Symanzik regulator it is an interesting choice as it does not affect directly local symmetries.

Far more general cutoff choice have been considered in the literature for specific purposes as well as for studies of the regulator dependences of the results. For example, in [10] a so-called compactly supported smooth regulator function was introduced which reproduces various well established regulators in certain limits of its parameters. In chapter ?? we shall come back to this issue.

In summary this leaves us with the following situation: For large cutoffs $k \rightarrow \Lambda$ with Λ being far larger than any physics scale, the effective action Γ_k tends towards the classical action or rather the UV-relevant part of the effective action. In renormalisable or more precisely asymptotically free theories this is a simple well-defined input. In turn, for $k \rightarrow 0$ we arrive at the full effective action $\Gamma = \Gamma_0$. Accordingly, with a well-defined initial condition and the flow $\partial_k \Gamma_k$ we can solve the theory.

Before we derive the flow equation, we briefly discuss the finiteness of the expressions dealt with here. So far we have used formal path integral manipulations. While we can always -implicitly- resort to a regularised version of the path integral so far indicated with $[d\varphi]_{\text{ren}}$, the potential interference of the additional regularisation with the underlying implicit regularisation calls for some caution. This fact is very apparent for the Callan-Symanzik regulator discussed above, but the issue is also present in the general case.

To avoid any of these subtleties we resort to a bootstrap approach: Assume for the time being that the theory is well-defined, and allows for the definition of a well-defined generating functional. More formally we have

- (1) $Z[J]$ is a *finite, renormalised* generating functional of the *finite, renormalised* correlation functions $G_n = \langle \varphi(x_1) \cdots \varphi(x_n) \rangle$.
- (2) It is differentiable, $\delta^n / \delta J^n Z$ exists for all n .

The property (1) is nothing but the existence of the quantum theory under considerations in terms of the correlation functions G_n . Note that we could even take a field φ which is not the fundamental field, see [6]. Property (2) implies that the field variable φ is a globally well-defined choice for a field. Note that this question is potentially relevant in theories where the effective degrees of freedom differ greatly from the fundamental fields.

With the properties (1) and (2) we are in the position to define the infrared regularised generating functional Z_k with

$$Z_k[J] = e^{-\Delta S_k[\frac{\delta}{\delta J}]} Z[J]. \quad (1.74)$$

Using the path integral representation (1.2) for $Z[J]$ by ignoring the renormalisation subtleties, and applying the relation

$$e^{-\Delta S_k[\frac{\delta}{\delta J}]} e^{\int d^d x J(x)\varphi(x)} = e^{-\Delta S_k[\varphi]} e^{\int d^d x J(x)\varphi(x)} \quad (1.75)$$

we arrive at (1.67). However, in view of renormalisation subtleties the representation (1.74) is advantageous as it disentangles the k -dependence and the underlying UV-renormalisation of the theory. Moreover, for the derivation of symmetry identities and further algebraic relations and constraints (1.74) is very well-suited.

Now we proceed with the derivation of the flow equation. The logarithmic scale derivative of the generating functional is given by

$$\begin{aligned} k \partial_k Z_k[J] &= -\frac{1}{2} \Delta S_k \left[\frac{\delta}{\delta J} \right] \underbrace{e^{-\Delta S_k[\frac{\delta}{\delta J}]} Z[J]}_{Z_k[J]} \\ &= -\frac{1}{2} \int \frac{d^d p}{(2\pi)^d} \frac{\delta}{\delta J(p)} \left[\partial_k R_k(p^2) \right] \frac{\delta}{\delta J(-p)} Z_k[J]. \end{aligned} \quad (1.76)$$

This leads us to the final flow equation for the generating functional Z ,

$$k \partial_k Z_k[J] = -\frac{1}{2} \int \frac{d^d p}{(2\pi)^d} \frac{\delta^2 Z_k[J]}{\delta J(p) \delta J(-p)} \partial_k R_k(p^2). \quad (1.77)$$

Eq. (1.77) is a closed functional integro-differential equation for J and resembles closely the heat equation with the Laplacian $\delta^2 / \delta J^2$. In terms of correlation functions it reads

$$k \partial_k \mathcal{Z}_k[J] = -\langle k \partial_k \Delta S_k[\varphi] \rangle \mathcal{Z}_k[J]. \quad (1.78)$$

Note also that the flow (1.77) is a generalised Callan-Symanzik equation, [7, 8, 9]. The latter has been derived with The Callan-Symanzik regulator $R_k(p^2) = k^2$, see (1.73).

From the flow of the generating functional \mathcal{Z}_k that of the Schwinger functional $\mathcal{W}_k = \ln \mathcal{Z}_k$ follows immediately. We simply need

$$\partial_k \mathcal{W}_k = \frac{1}{\mathcal{Z}_k} \partial_k \mathcal{Z}_k, \quad \frac{1}{Z_l[J]} Z_k^{(2)}[J] = \mathcal{W}_k^{(2)}[J] + (\mathcal{W}_k^{(1)}[J])^2. \quad (1.79)$$

Inserting (1.79) in (1.77) leads us directly to

$$\partial_t \mathcal{W}_k[J] = -\frac{1}{2} \int \frac{d^d p}{(2\pi)^d} \left[\mathcal{W}_k^{(2)}[J] + (\mathcal{W}_k^{(1)}[J])^2 \right] \partial_t R_k(p^2), \quad t = \ln k/k_{\text{ref}}. \quad (1.80)$$

In (1.80) we have introduced the RG-time t with some reference scale k_{ref} . The standard choice for k_{ref} is the initial UV cutoff Λ or some physics scale such as the mass gap of the theory. In QCD it is suggestive to use Λ_{UV} . Eq. (1.80) is related to the Polchinski equation for the Wilson effective action. The latter generates amputated connected correlation functions and is obtained from the Schwinger functional with $J \simeq \mathcal{P}\phi$, where \mathcal{P} is the classical dispersion and ϕ is the Wilsonian (infrared) field, for more details see [6] and references therein.

Finally we aim at the effective action Γ_k defined in (1.68) as the modified Legendre transform of \mathcal{W}_k . We take the t -derivative of the right hand side of (1.68) and find

$$\begin{aligned} \partial_t \Gamma_k[\phi] &= \int d^d x \partial_t J(x) \phi(x) - \partial_t \mathcal{W}_k[J] - \int d^d x \frac{\delta \mathcal{W}_k}{\delta J(x)} \partial_t J(x) - \partial_t \Delta S_k[\phi] \\ &= \frac{1}{2} \text{Tr} (G_k + \langle \varphi \rangle^2) \partial_t R_k - \partial_t \Delta S_k[\phi] = \frac{1}{2} \text{Tr} G_k \partial_t R_k. \end{aligned} \quad (1.81)$$

where G_k is the full propagator,

$$G_k = \mathcal{W}_k^{(2)} = \frac{1}{\Gamma_k^{(2)} + R_k}. \quad (1.82)$$

In (1.81) we used (1.6) to find that the first and the third term on the right hand side of the first line are equal (up to a sign). The insertion of (1.80) then leads to the second line. Eq. (1.82) can be used to express the full scale-dependent propagator in terms of the effective action. Using (1.82) in (1.81) leads us to the Wetterich equation [11],

$$\partial_t \Gamma_k[\phi] = \frac{1}{2} \text{Tr} \frac{1}{\Gamma_k^{(2)} + R_k} \partial_t R_k = \frac{1}{2} \int \frac{d^d p}{(2\pi)^d} \frac{1}{\Gamma_k^{(2)}(p, -p) + R_k(p^2)} \partial_t R_k(p^2). \quad (1.83)$$

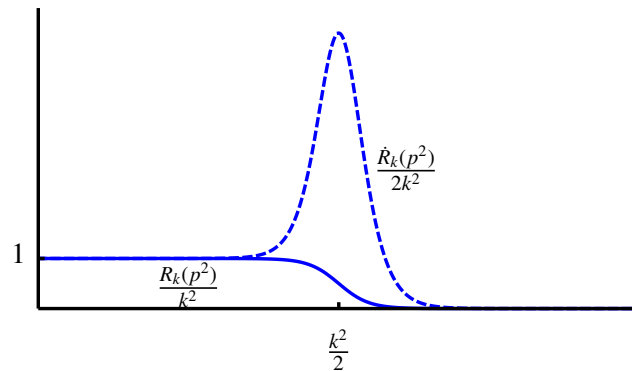


Figure 1.6: The regulator function depicted in Fig. 1.5 and its derivative with respect to the RG time $t = \ln(k/k_0)$.

Beginning of the 90ties groups have been working on functional renormalisation group equations for the different manifestations of the generating functionals. In the context of the flow equation for the scale-dependent effective action, (1.83), we would like to mention the work of Bonini, D’Attanasio and Marchesini [12] where essentially this equation was derived independently and shortly after [11]. Further initial development has been achieved by Ellwanger [13], Morris [14] and Becchi [15]. The Wegner-Houghton equation of the seminal paper [16] is obtained from (1.83) with the sharp cutoff given in (1.73). The Callan-Symanzik equation in the form Symanzik introduced, [8, 9], is nothing but (1.83) with $R_k = k^2$. There also more general choice are briefly mentioned. More details and references can be found in [6].

The general form of the cutoff introduced in [11] has finally allowed for multifaceted applications of these kind of flow equations. Eq. (1.83) is the central tool of these notes and therefore we summarise its most important features before proceeding with the discussion of practical issues as diagrammatic representation and applications.

Recapitulating the properties of the regulator function and inspecting the structure of (1.83) one realizes the following facts:

- * The flow of the effective average action Γ_k is regulator-dependent. However the effective action $\Gamma_{k \rightarrow 0}$ does not depend on the regulator since the latter vanishes at low energies.
- * During the flow all possible interaction terms in accord with the symmetries are produced. Therefore Γ_k contains an infinite sum of terms. Most practical applications then require a truncation of this infinite sum, as discussed in the following section.
- * Finiteness for the flow equation of the 1PI effective action in the UV as well as in the IR is guaranteed by the limits of the regulator function. This can be seen from

$$\frac{1}{\Gamma_k^{(2)}[\phi_c] + R_k(p^2)} \xrightarrow{p^2/k^2 \rightarrow 0} \frac{1}{\Gamma_k^{(2)}[\phi_c] + k^2}, \quad \frac{1}{\Gamma_k^{(2)}[\phi] + R_k(p^2)} \partial_t R_k(p^2) \xrightarrow{p^2/k^2 \rightarrow \infty} 0. \quad (1.84)$$

- * The regulator may break symmetries, and in particular gauge symmetries. Relevant examples are
 - (a) chiral symmetry
 - (b) Lorentz symmetry
 - (c) non-Abelian gauge symmetry in Quantum Chromodynamics
 - (d) diffeomorphism invariance in gravity.

If these symmetries are assumed to hold on the quantum level its conservation during the flow has to be realized separately. This can be done with modified Ward-Takahashi or Slavnov-Taylor identities as detailed in section ?? or with the background field method introduced in subsection ?. The latter method will then be used in chapter ?? within QCD and in chapter ?? in the context of Quantum Einstein Gravity.

- * The flow equation for the scale-dependent effective action $\Gamma_k[\phi]$ together with the initial condition $\bar{\Gamma}_\Lambda[\phi]$ at the cutoff scale $k = \Lambda$ provides the definition of the quantum field theory in terms of the effective action $\Gamma_{k \rightarrow 0}$. In the presence of a Gaussian or non-Gaussian ultraviolet fixed point the UV cutoff can be taken to infinity, $\Lambda \rightarrow \infty$. In these cases the respective theory is globally defined up to arbitrary high energy scales. While in QCD this scenario is ensured due to asymptotic freedom (Gaussian fixed point), this is the idea underlying the Asymptotic Safety scenario, [17]. The latter is discussed in chapter ??.

$$\partial_t \Gamma_k[\phi] = \frac{1}{2} \text{Diagram 1}$$

$$\partial_t \Gamma_k^{(2)}[\phi] = -\frac{1}{2} \frac{\delta}{\delta \phi} \text{Diagram 2} = -\frac{1}{2} \text{Diagram 3} + \text{Diagram 4}$$

Figure 1.7: Upper panel: Diagrammatic representation of the Wetterich equation (1.83).
Lower panel: Diagrammatic representation of the flow equation for the two-point function.

In order to get a better understanding of the important equation (1.83) we can depict it in a diagrammatic way as shown in the upper panel of Fig. 1.7. We use the line with a filled circle for the full propagator $(\Gamma_k^{(2)} + R_k)^{-1}$ (not to be confused with the one used within the DSEs) and introduced the regulator insertion $\partial_t R_k$ with a crossed circle. Notably, (1.83), is an exact equation with a one-loop structure in contradistinction to the DSE, see also the diagrammatic representations of the FRG, Fig. 1.7, and DSE, Fig. 1.2, respectively. The flow equation for any n -point function can be obtained by taking the n -th derivative of the Wetterich equation with respect to the fields. As an example the diagrammatic equation for the two-point function is given in the lower panel of Fig. 1.7. Realising the fact that classical propagators and vertices do not appear we will drop the blobs in most diagrammatic representations to indicate the dressed quantities in the following. There is no need for distinction in contrast to the diagrammatic representation of the DSEs where we have dressed and bare quantities and in consequence have to make clear which quantities are involved.

Before we go on to the practical issues like truncation schemes in the following sections let us briefly compare the discussion of this section to the one of the previous section 1.3. The attentive reader still waits for the field renormalization and rescaling performed in the previous section but ignored so far within the FRG framework. Here, we will not go into the details and refer the interested reader to e.g. [6, 18, 19]. Instead, we will use the observation made in (1.54). Having obtained the flow equation for a coupling extracted from the Wetterich equation one can obtain the running which accounts for the correct field redefinition and rescaling by applying the scale derivative to the coupling modified by a suitable power of the RG scale k (according to the couplings dimension) and a suitable power of the wave function renormalization (according to the number of fields involved in the corresponding interaction). We will come back to this issue during the discussion of renormalization group fixed points in section ??.

1.5 Truncation schemes

Summarizing the last section, we have seen that a theory at a given scale k can be described by the effective average action $\Gamma_k[\phi]$. The latter one interpolates between the classical action $S[\phi]$ at high energies $k \rightarrow \infty$ and the full quantum effective action $\Gamma[\phi]$ at low energies $k \rightarrow 0$. This interpolation is described by the Wetterich equation (1.83). While integrating out the quantum fluctuations, which means flowing from high to low energies, new couplings might be produced which have to be added to those present at the classical level.³ Thus the effective average action consists of all combinations of the fields and their derivatives which satisfy the underlying symmetries of the theory.⁴ In a very abstract way we can write

$$\Gamma_k[\phi] = \sum_n g_n \mathcal{O}_n[\phi, \partial_\mu \phi] \quad (1.85)$$

where g_n are the coupling constants and \mathcal{O}_n are operators constructed from the fields and their derivatives. Since we have to deal with an infinite sum we cannot solve the Wetterich equation at once. Although the latter is an exact equation we have to truncate it in order to make it numerically (or even analytically) accessible. This is the main and most important approximation used within the FRG framework.

According to (1.85), Γ_k depends on the coupling constants, the fields and their derivatives. This already suggests three truncations schemes:

1. An expansion in the coupling constants which translates into a loop expansion is related to ordinary perturbation theory.
2. An expansion in powers of the fields is called a vertex expansion.
3. The derivative expansion sorts the terms in Γ_k according to their numbers of derivatives.

Within the rest of the section we explain these three truncation schemes in general and afterwards discuss all of them at the example of a zero-dimensional toy model.

1.5.1 Loop Expansion

Renormalized perturbation theory to any order can be easily computed from the flow equation within an iterative procedure. This approach is also amiable towards computer-algebra implementation and is a simple way to generate perturbative 1PI diagrams to any order including the combinatorial factors. Here we illustrate this at one-loop and two-loop perturbation theory. See [20] for more details.

First, we write the effective action within a loop expansion

$$\Gamma_k^{N\text{-loop}} = S + \sum_{n=1}^N \Delta\Gamma_k^{n\text{-loop}}, \quad \Gamma_k = \lim_{N \rightarrow \infty} \Gamma_k^{N\text{-loop}} \quad (1.86)$$

where S is the classical action and $\Delta\Gamma_k^{n\text{-loop}}$ comprises the quantum corrections at n -th loop order. Let us consider our simple exemplary scalar theory. Inserting the ansatz (1.86) into the Wetterich equation and restricting to one-loop order we find

$$\partial_t \Gamma_k^{1\text{-loop}}[\phi] = \frac{1}{2} \text{Tr} \frac{1}{\Gamma_k^{(2)}[\phi] + R_k} \partial_t R_k \Big|_{1\text{-loop}} = \frac{1}{2} \text{Tr} \frac{1}{S^{(2)}[\phi] + R_k} \partial_t R_k = \frac{1}{2} \text{Tr} \left(\partial_t \ln [S^{(2)}[\phi] + R_k] \right). \quad (1.87)$$

³In terms of the simple scalar theory this will be discussed in subsection 1.5.2.

⁴Actually, this is only true as long as the regulator is symmetric. For more details see the discussion of the modified Ward-Takahashi identity, (??), in section ??.

We have dropped all quantum corrections in $\Gamma_k^{(2)}$ on the right hand side of (1.87) as they contribute only to higher loop orders. The reason for that is the fact that the Wetterich equation itself has a one-loop structure. This can be seen immediately since the trace contributes only a one-loop integration and further loops, which might appear within the expansion (1.86), are neglected. Note also that in general the trace Tr and the cutoff derivative ∂_t do not commute, as $\text{Tr} \ln(S^{(2)} + R_k)$ requires a UV-renormalization, while the expression in (1.87) is finite. This already hints at the fact that the t -integration together with the initial effective action Γ_Λ provides for the UV-renormalisation.

Now we integrate (1.87) over momentum from a fixed cutoff Λ down to the momentum shell with momentum k to gain

$$\Gamma_k^{1\text{-loop}}[\phi] = \frac{1}{2} \text{Tr} \left\{ \ln(S^{(2)}[\phi] + R_k) - \ln(S^{(2)}[\phi] + R_\Lambda) \right\} + \Gamma_\Lambda^{1\text{-loop}}[\phi]. \quad (1.88)$$

Note that only the trace of the difference in (1.88) is finite. The second term under the trace at $k = \Lambda$ is nothing but the subtraction term that renders the effective action finite. It is reminiscent of the Pauli-Villars regularization where a divergent diagram is made finite by subtracting the same diagram with the particle's propagator replaced by the one of a fictitious heavy particle.

Fixing now $k = 0$ we can use the fact that the regulator R_k vanishes at $k = 0$ and evaluate the derivative of (1.88) with respect to Λ to find

$$\Lambda \partial_\Lambda \Gamma^{1\text{-loop}} = \Lambda \partial_\Lambda \Gamma_\Lambda^{1\text{-loop}} - \frac{1}{2} \text{Tr} \frac{1}{S^{(2)} + R_\Lambda} \Lambda \partial_\Lambda R_\Lambda. \quad (1.89)$$

The right hand side of Eq. (1.89) vanishes due to the flow equation for $\Gamma_\Lambda^{1\text{-loop}}$. This shows the cutoff independence of the one-loop effective action, $\Gamma^{1\text{-loop}}$. According to (1.88) the latter one is given as

$$\Gamma^{1\text{-loop}}[\phi] = \frac{1}{2} \text{Tr} \left\{ \ln(S^{(2)}[\phi]) - \ln(S^{(2)}[\phi] + R_\Lambda) \right\} + \Gamma_\Lambda^{1\text{-loop}}[\phi]. \quad (1.90)$$

and carries no dependence on Λ due to (1.89). Thus, the limit $\Lambda \rightarrow \infty$ can be taken.

In order to obtain a flow equation within the two-loop approximation we have to take into account the one-loop quantum correction $\Delta\Gamma_k^{1\text{-loop}}$ of our expansion (1.86) on the right hand side of the flow equation (1.83):

$$\begin{aligned} \partial_t \Gamma_k^{2\text{-loop}}[\phi] &= \partial_t \Gamma_k^{1\text{-loop}}[\phi] + \partial_t \Delta\Gamma_k^{2\text{-loop}}[\phi] \\ &= \frac{1}{2} \text{Tr} \frac{1}{\Gamma_k^{(2)}[\phi] + R_k} \dot{R}_k \Big|_{2\text{-loop}} = \frac{1}{2} \text{Tr} \frac{1}{S^{(2)}[\phi] + \Delta\Gamma_k^{1\text{-loop}(2)}[\phi] + R_k} \dot{R}_k \Big|_{2\text{-loop}} \\ &= \frac{1}{2} \text{Tr} \frac{1}{S^{(2)}[\phi] + R_k} \dot{R}_k - \frac{1}{2} \text{Tr} \frac{1}{S^{(2)}[\phi] + R_k} \Delta\Gamma_k^{1\text{-loop}(2)}[\phi] \frac{1}{S^{(2)}[\phi] + R_k} \dot{R}_k. \end{aligned} \quad (1.91)$$

Note that the first part in the last line comprises $\partial_t \Gamma_k^{1\text{-loop}}$, and the second part includes the two-loop term. For the computation of (1.91) we need $\Delta\Gamma_k^{1\text{-loop}(2)}$ which can be derived from (1.88) by taking two field derivatives. We arrive at

$$\Delta\Gamma_k^{1\text{-loop}(2)} = \frac{1}{2} \left(\text{Tr} \frac{1}{S^{(2)} + R_k} S^{(4)} - \text{Tr} \frac{1}{S^{(2)} + R_k} S^{(3)} \frac{1}{S^{(2)} + R_k} S^{(3)} \right)_\Lambda^k + \Delta\Gamma_\Lambda^{1\text{-loop}(2)}, \quad (1.92)$$

and a graphical representation of (1.92) is depicted in Fig. 1.8. Inserting this result into (1.91) we obtain a flow equation which can be integrated from a cutoff scale Λ down to $k = 0$. With this we obtain the sought-after $\Gamma^{2\text{-loop}}$. As in the one-loop case the initial effective action has a two-loop contribution

$$\Gamma_{k,1\text{-loop}}^{(2)} - \Gamma_{\Lambda,1\text{-loop}}^{(2)} = \frac{1}{2} \left(\text{Diagram 1} \right) - \frac{1}{2} \left(\text{Diagram 2} \right)$$

Figure 1.8: Upper panel: Graphical representation of (1.92).

Lower panel: Graphical representation of the subtracted diagrams (double lines). The scale dependence of the perturbative propagator (full line) is due to the regulator term R_k , hence the index k or Λ .

$\Gamma_{\Lambda}^{2\text{-loop}}$ whose Λ -dependence cancels that of the integrated flow. This is guaranteed by Γ_{Λ} satisfying the flow equation (1.83) leading to

$$\Lambda \partial_{\Lambda} \Gamma[\phi] = 0, \quad (1.93)$$

that is *RG-consistency* of the theory, the independence of the UV cutoff Λ .

The above procedure is reminiscent of the formalism invented by Bogoliubov, Parasiuk, Hepp and Zimmermann (BPHZ) allowing for rigorous proofs of perturbative renormalizability. First, the divergences appearing in subgraphs are healed in (1.92) as depicted in Fig. 1.8. The finite result is then replacing the divergent subgraph and the full two-loop contribution can be healed with appropriate subtractions (integrated version of (1.91)). It is a more general procedure than the original BPHZ renormalization as the subtractions carry a general momentum and field dependence.

This already indicates that the comparison of RG-schemes as induced by the functional renormalisation group, and standard perturbative schemes such as the $\overline{\text{MS}}$ -scheme or lattice RG-schemes is in general difficult. A detailed discussion of this issue goes beyond the scope of this lecture course, for details see e.g. [21, 22, 23, 20, 6, 18, 24] and literature therein.

1.5.2 Vertex Expansion

Within the last subsection we have seen that the Wetterich equation and its evaluation can be reduced to the well-known perturbative treatment, i.e. an expansion which works very well for small couplings. However, the strength of the Wetterich equation is not limited to the weak-coupling regime. In order to profit from this fact we will now discuss an alternative truncation, the so-called vertex expansion.

In the vertex-expansion scheme, the effective average action Γ_k is expanded in the number of external fields, n . Considering again our simple scalar example and expanding about a general background field $\bar{\phi}(x)$ leads to

$$\Gamma_k[\phi] = \sum_{n=0}^{\infty} \frac{1}{n!} \int d^d x_1 \dots d^d x_n \Gamma_k^{(n)}[\bar{\phi}](x_1, \dots, x_n) (\phi(x_1) - \bar{\phi}(x_1)) \dots (\phi(x_n) - \bar{\phi}(x_n)), \quad (1.94)$$

with the 1PI vertices $\Gamma_k^{(n)}[\bar{\phi}]$. Note that in a Z_2 -symmetric theory (invariance under $\phi \rightarrow -\phi$) all odd vertices vanish identically if evaluated on a vanishing background. During the flow no ϕ -odd terms will be generated. More details on symmetries and flow equations can be found in section ???. Very often the vertex expansion is done in momentum space. In this case the fields depend on momenta p instead of spacetime points x . Therefore the 1PI vertices $\Gamma^{(n)}(p_1, \dots, p_{n-1})$ will depend on $(n - 1)$ momenta where the momentum conservation is already taken into account. Thus, the two-point vertex for example carries the full momentum dependence of the propagator. In other words, The vertex expansion is the expansion scheme most suitable for the investigation of momentum dependencies of correlation functions. Employing the expansion (1.94) for the left and right hand side of the Wetterich equation, (1.83), we end up with a tower of coupled differential equations for the 1PI n -point vertices, with $n = 0, 1, \dots, \infty$. The first equations of that tower read

$$\begin{aligned}
\partial_t \Gamma_k^{(0)}[\bar{\phi}] &= \frac{1}{2} \text{Tr} \frac{1}{\Gamma_k^{(2)} + R_k} \dot{R}_k, \\
\partial_t \Gamma_k^{(1)}[\bar{\phi}] &= -\frac{1}{2} \text{Tr} \frac{1}{\Gamma_k^{(2)} + R_k} \Gamma_k^{(3)} \frac{1}{\Gamma_k^{(2)} + R_k} \dot{R}_k, \\
\partial_t \Gamma_k^{(2)}[\bar{\phi}] &= -\frac{1}{2} \text{Tr} \frac{1}{\Gamma_k^{(2)} + R_k} \Gamma_k^{(4)} \frac{1}{\Gamma_k^{(2)} + R_k} \dot{R}_k + \text{Tr} \frac{1}{\Gamma_k^{(2)} + R_k} \Gamma_k^{(3)} \frac{1}{\Gamma_k^{(2)} + R_k} \Gamma_k^{(3)} \frac{1}{\Gamma_k^{(2)} + R_k} \dot{R}_k, \\
&\vdots \qquad \qquad \qquad \vdots
\end{aligned} \tag{1.95}$$

where a pictorial representation of the third line can be found in the lower panel of Fig. 1.7. This tower of coupled differential equations is reminiscent of the tower of DSEs discussed in section 1.2. Similar to the situation encountered there we can see in (1.95) that the flow equation for the 1PI n -point function depends on the 1PI $(n + 2)$ -point function. Despite the similarities of DSE and FRG there are also relevant differences in terms of the resummation schemes induced within a certain approximation to the effective action: First of all the coupled FRG-tower (1.95) is one-loop exact and only depends on fully dressed vertices and propagators $\Gamma^{(n)}$. Moreover it does not require any UV-renormalisation as discussed before. The price to pay for these features is the dependence on the RG-time t , in its integrated form (over t) the FRG can indeed be understood as a $d + 1$ dimensional one-loop exact DSE. Still, also in its $d + 1$ -dimensional DSE form, the UV-renormalisation is already taken care of.

Of course this does not help to solve the infinite tower and thus the set of flow equations has to be truncated. This can be either done by dropping all the higher vertices, relating them to lower ones by means of symmetry relations, or using some initial k -independent value. In all these cases the generation of new terms during the flow (see footnote 3) has to be suppressed.

Most importantly in non-perturbative cases there is no small parameter involved in this or other systematic approximation schemes. This makes it hard to control the error of the approximation. A discussion of the control of the systematic error is given in ???. Here we only mention that diagrams with higher order vertices are usually phase-space suppressed. This phase space suppression is generically very strong, but in case of resonant interactions and large density it may be delayed to even higher orders, or it may even not be present for a subset of vertices. In QCD both scenarios are relevant: For low energies we encounter resonant momentum channels in the four-quark interactions (scalar and pseudo-scalar) that signal the onset of chiral symmetry breaking and hadronisation. Moreover, finite density QCD is one of the most interesting applications of functional methods as they have no sign problem.

1.5.3 Derivative Expansion

A third, and commonly used, approximation scheme is the derivative expansion. In order to understand the idea behind let us restate the Wetterich equation (1.83) in momentum-space notation and split its

right hand side into two parts according to

$$\partial_t \Gamma_k[\phi] = \frac{1}{2} \int_{q^2 \lesssim k^2} \frac{d^d q}{(2\pi)^d} \frac{1}{\Gamma_k^{(2)} + R_k} \dot{R}_k + \frac{1}{2} \int_{q^2 \gtrsim k^2} \frac{d^d q}{(2\pi)^d} \frac{1}{\Gamma_k^{(2)} + R_k} \dot{R}_k. \quad (1.96)$$

The regulator and its t -derivative have to decay for $p^2/k^2 \rightarrow \infty$, see (1.72b), the second term can be neglected as the integrand is $\dot{R}_k(q^2)$ in the area $q^2 \gtrsim k^2$. This suppression is more efficient the more rapid \dot{R}_k decays for $q^2/k^2 \rightarrow \infty$. Note that the general functional optimisation criteria discussed in ?? require rapidly decaying regulators.

Hence we are left with the first term in (1.96). Furthermore we restrict ourselves to fields that probe the infrared regime of the theory. In momentum space this reads

$$\phi(p^2 \gtrsim k^2) \approx 0. \quad (1.97)$$

Then $\Gamma^{(2)}[\phi]$ is only probed for momenta $p^2 \lesssim k^2$. This can be made even more explicit by resorting to the vertex expansion again and taking all external momenta $p_i^2 \lesssim k^2$. Then, all momenta p in vertices and propagators are restricted by k . Since $p^2 \lesssim k^2$ is the infrared-suppressed regime, we do not expect large momentum dependences. Consequently an expansion about $p^2 = 0$ should work well. This is the derivative expansion.

Let us now discuss some of its properties within our standard the scalar example of a real scalar ϕ^4 -theory. This theory has a Z_2 -symmetry under $\phi \rightarrow -\phi$. The aforementioned expansion in powers of momenta translates into an expansion in powers of derivatives. Thus we sort the terms appearing in the effective average action accordingly. The first two orders are given by

$$\Gamma_k[\phi] = \int d^d x \left(V_k[\rho] + \frac{1}{2} Z_k[\rho] \partial_\mu \phi \partial^\mu \phi + \mathcal{O}(\partial^4) \right), \quad (1.98)$$

where we defined $\rho = 1/2 \phi^2$ for convenience. Using (1.98) the Wetterich equation again turns into a tower of differential equations. The first two equations of this tower are the flow equations for the effective average potential $V_k[\rho]$ (which becomes the effective potential for $k \rightarrow 0$) and for the ρ -dependent wave function renormalization $Z_k[\rho]$. These read

$$\begin{aligned} \partial_t V_k(\rho_0) &= \frac{1}{2 \text{Vol}_d} \text{Tr} \frac{1}{\Gamma_k^{(2)} + R_k} \dot{R}_k \Big|_{\phi(x)=\phi_0}, \\ \partial_t Z_k(\rho_0) &= \frac{1}{2 \text{Vol}_d} \frac{\partial}{\partial p^2} \left(\frac{\delta}{\delta \phi(-p)} \frac{\delta}{\delta \phi(q)} \text{Tr} \frac{1}{\Gamma_k^{(2)} + R_k} \dot{R}_k \Big|_{\phi(x)=\phi_0, p=q} \right)_{p=0}, \\ &\vdots \qquad \qquad \qquad \vdots \end{aligned} \quad (1.99)$$

where we restricted ourselves to the homogeneous case, $\phi(x) = \phi_0 = \text{const}$ and $\rho_0 = 1/2 \phi_0^2$ and Vol_d denotes the spacetime volume $\int d^d x$. Note that this system of flow equations is coupled as well since $\Gamma_k^{(2)}$ on the right hand side contains arbitrary high orders in the derivative expansion.

In order to solve this system we have to truncate the series in (1.98) at some point. The frequently used lowest order uses $Z_k[\rho] = 1$ and neglects all higher order terms. It is called local potential approximation (LPA). An $O(N)$ -symmetric scalar field theory is discussed in detail for this approximation in appendix 2.3. Very often, as a higher order contribution a scale-dependent but field-independent wave function renormalization Z_k is considered. This approximation is called LPA'.

Let us for a moment stick to the effective average potential $V_k[\phi]$ and its limit for $k \rightarrow 0$, the effective potential $V[\phi]$. One reason for the interest in them is their role as an important indicator for spontaneous

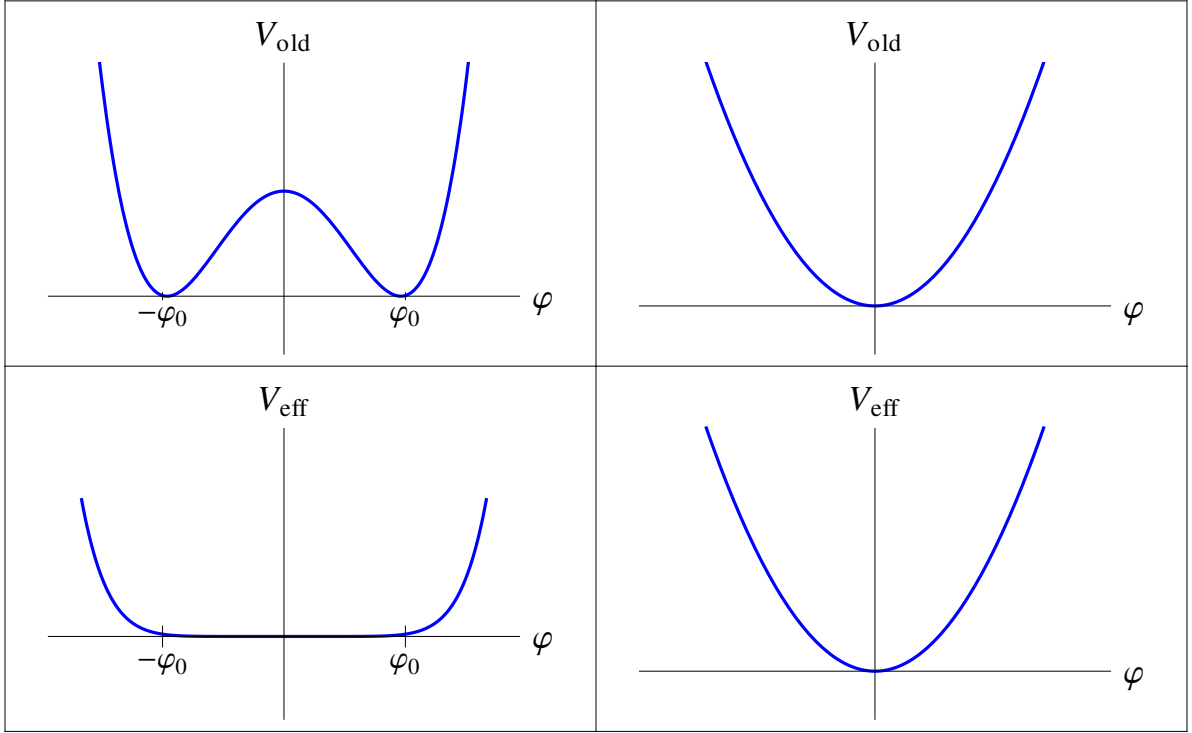


Figure 1.9: The classical initial potential V_Λ (upper panel) and the associated effective potential $V_{k=0}$ (lower panel) for a spontaneously broken symmetry (left hand side) and for unbroken symmetry (right hand side).

symmetry breaking. The number of minima depends on the theories phase, the symmetric or the symmetry broken one (for illustration see Fig. 1.9). To be more precise let us consider a classical potential $V_\Lambda[\phi] = \frac{1}{2}m_\Lambda^2\phi^2 + \frac{\lambda_\Lambda}{4!}\phi^4$ with positive m_Λ^2 and positive λ_Λ . A sketch of it is depicted in the upper right plot of Fig. 1.9. Integrating out the quantum fluctuations i.e. lowering the scale k from $k = \Lambda$ to $k = 0$ we find the effective potential. Assuming the quantum fluctuations not to break the symmetry the effective potential will have a similar form as the classical one (see lower right plot of Fig. 1.9). Now let assume the symmetry to be broken spontaneously at $k = \Lambda$ (see upper left plot in Fig. 1.9). What does the effective potential will look like under the assumption, that the symmetry is not restored by the quantum fluctuations? Using a constant background field ϕ_0 at $k = 0$, the quantum EoM, (1.7), at vanishing source field $J(x) = 0$ reduces to

$$\frac{\delta\Gamma[\phi]}{\delta\phi(x)} = 0 \quad \Rightarrow \quad \frac{\partial V_{k=0}(\phi_0)}{\partial\phi_0} = 0. \quad (1.100)$$

As discussed below (1.7) the 1PI effective action reduces to the free energy in this case and therefore represents an extensive quantity. Thus the effective potential $V_{k=0}(\phi_0)$ has to be convex and it can be seen as an analogue to the Maxwell construction for the thermodynamic free energy. Therefore the effective potential flattens compared to the classical one in the symmetry broken phase (see lower left plot in Fig. 1.9). This will be explained in more detail in the example in appendix 2.3.

This quick excursion to the effective average potential already shows that the derivative expansion is a powerful tool for investigating symmetry breaking mechanisms and critical phenomena. This will be used in chapter ?? e.g. when discussing spontaneous chiral symmetry breaking.

1.5.4 Zero-Dimensional Toy Model

In the following we illustrate the different approximation and truncation schemes introduced above with the help of a zero-dimensional toy-model quantum field theory, which was also discussed in [25, 26, 27]. The zero-dimensional theory lends itself as an example for a detailed discussion, since calculations can be clearly laid out. Furthermore, since the full integrals are numerically solvable, we can compare the results of the applied truncation strategies with the numerical result and therefrom estimate their quality. Apart from that the toy model is interesting on its own rights as it can be thought of as a lattice gauge theory defined at one lattice site, or a quantum-mechanical theory at high temperatures. A more detailed explanation of these applications can be found in [25, 27].

As discussed in detail in section 1.4 the starting point of our investigation is the regulator-dependent generating functional of the theory. The zero-dimensional toy model to be discussed here depends on a scalar field φ (at one spacetime point) and satisfies the Z_2 symmetry (invariance under $\varphi \rightarrow -\varphi$). Note that in zero dimensions the scale k can be compared with the regulator R trivially. Thus the regulator-dependent generating functional reads

$$Z_R(J) = \int d\varphi \exp\left(-S(\varphi) - \frac{1}{2} R \varphi^2 + J \varphi\right), \quad \text{with} \quad S(\varphi) = \frac{1}{2} \varphi^2 + \frac{\lambda}{4!} \varphi^4. \quad (1.101)$$

The full generating functional, including all quantum fluctuations, is obtained at $R = 0$. Depending on the source J it is numerically or even analytically (for $J = 0$) solvable. By Legendre transforming the Schwinger functional $W_R(J) = \ln(Z_R(J))$, we end up with the effective average action

$$\Gamma_R(\phi) = \sup_J (J\phi - W_R(J)) - \frac{1}{2} R \phi^2, \quad (1.102)$$

and the flow equation

$$\partial_R \Gamma_R = -\partial_R W_R - \partial_R \left(\frac{1}{2} R \phi^2\right) = \frac{1}{2} \left(\partial_\phi^2 \Gamma_R + R\right)^{-1}. \quad (1.103)$$

In order to solve the flow equation, we still need to specify the UV initial condition $\Gamma(\phi, R = \Lambda)$ and the boundary conditions $\Gamma(\phi = \pm\infty, R)$. We will do so while discussing different truncation schemes in the following subsections.

Iterative Solution

The first solution strategy encountered above was the loop expansion. Within zero dimensions there is no propagation and therefore it is not straight forward to count loops. Nevertheless, one could reinstall the \hbar as a loop counting factor into the equations, which is not done here. Instead, we follow the strategy detailed above, which turns into an iterative solution of the flow equation (1.103). We can use the classical action in (1.101) as a starting point and insert it into the right hand side of the flow equation. The resulting effective average action $\Gamma_R^{1\text{st order}}$ can then be used as a renewed input for the right hand side of the flow equation. These steps are repeated until the resulting effective action is converged to a final solution. For the first iteration step we obtain

$$\partial_R \Gamma_R^{1\text{st order}}(\phi) = \frac{1}{2} \frac{1}{\partial_\phi^2 S(\phi) + R} = \frac{1}{2} \frac{1}{1 + \frac{1}{2} \phi^2 + R}. \quad (1.104)$$

This flow equation can be integrated analytically and leads to the "1-Loop effective average action"

$$\Gamma_R^{1\text{st order}} = S(\phi) + \frac{1}{2} \ln\left(\partial_\phi^2 S(\phi) + R\right), \quad \text{with} \quad \Gamma_\Lambda^{1\text{st order}}(\phi) = S(\phi) + \frac{1}{2} \ln\left(\partial_\phi^2 S(\phi) + \Lambda\right). \quad (1.105)$$

In the second iteration step, the flow equation reads

$$\partial_R \Gamma_R^{2^{\text{nd}} \text{order}}(\phi) = \frac{1}{2} \frac{1}{\partial_\phi^2 \Gamma_R^{1^{\text{st}} \text{order}}(\phi) + R} = \frac{1}{2} \frac{1}{1 + R + \frac{\lambda}{2} \phi^2 + \frac{\lambda}{2} \frac{1+R-\frac{\lambda}{2} \phi^2}{(1+R+\frac{\lambda}{2} \phi^2)^2}}, \quad (1.106)$$

that can be integrated analytically as in the previous iteration step. This iterative procedure can be repeated, using numerical integration if necessary, to find higher iterative solutions $\Gamma_R^{n^{\text{th}} \text{order}}$. It turns out (see [27]) that this iterative procedure is very useful for $\phi \gtrsim 1$ but less precise for small ϕ .

Derivative Expansion

The zero-dimensional model simplifies various aspects of the calculation. One of them is the fact that in zero dimensions no propagation can occur and no derivatives can appear. This manifests itself in the non-existence of a standard kinetic term in the classical action (1.101). Most importantly this makes the lowest order in the derivative expansion, the LPA, exact.

For homogeneous field configurations, as it is the case in our zero dimensional model, Γ_R depends only on $|\phi|$, and we can introduce the effective average potential $V_R(\rho) = \Gamma_R(\phi)$ with $\rho = \phi^2/2$. Inspecting the flow equation (1.103) we find that we need the second variation of the effective average potential V_R

$$\partial_\phi^2 V_R(\rho) = V_R'(\rho) + V_R''(\rho) \phi^2. \quad (1.107)$$

Inserting this into the flow equation expressed in terms of the effective average potential V_R we find

$$\partial_R V_R(\rho) = \frac{1}{2} \left(\frac{1}{V_R'(\rho) + 2\rho V_R''(\rho) + R} \right) \quad (1.108)$$

Discretizing the effective average potential $V_R(\rho)$ now allows for a numerical solution of its flow equation. The result can be obtained to arbitrary precision, depending on the discretization.

Vertex Expansion

Instead of using this numerical method we can utilize an alternative approach. Following the explanations above we can solve the flow equation (1.103) by using a vertex expansion. Writing the effective average action Γ_R as a series in powers of the field ϕ via

$$\Gamma_R(\phi) = \sum_{n=0}^{\infty} \frac{\lambda_{2n}}{(2n)!} \phi^{2n}, \quad (1.109)$$

we find that this is an exact expansion if Γ_R is analytic around $\phi = 0$. Note that λ_{2n} depends on the regulator i.e. $\lambda_{2n} = \lambda_{2n}(R)$. In order to obtain the flow equations for the coupling constants λ_{2n} we have to project the flow equation (1.103) by a suitable power of derivatives with respect to the fields i.e.

$$\partial_R \lambda_{2n} = \frac{1}{2} \partial_\phi^{2n} \left. \frac{1}{\partial_\phi^2 \Gamma_R + R} \right|_{\phi=0}. \quad (1.110)$$

Figure 1.10: The effective action $\Gamma_{R=0}$ evaluated within the vertex expansion for various N_{\max} ranging from 3 to 10 compared to the numerically evaluated full result.

This leads to a tower of flow equations whose first equations are

$$\begin{aligned}
\partial_R \lambda_0 &= \frac{1}{2} \frac{1}{\lambda_2 + R}, \\
\partial_R \lambda_2 &= -\frac{1}{2} \frac{\lambda_4}{(\lambda_2 + R)^2}, \\
\partial_R \lambda_4 &= 3 \frac{\lambda_4^2}{(\lambda_2 + R)^3} - \frac{1}{2} \frac{\lambda_6}{(\lambda_2 + R)^2}, \\
&\vdots \qquad \qquad \qquad \vdots \qquad \qquad \qquad \vdots
\end{aligned} \tag{1.111}$$

Truncating this infinite tower of coupled differential equations by introducing a finite N_{\max} into the expansion of the effective action, (1.109), is equivalent to setting all couplings $\lambda_{2n} = 0$ for $n > N_{\max}$. With this truncation we can solve the tower of differential equations and find, as expected, that the Taylor expansion of the generating functional describes the full functional well for $\phi \ll 1$, but becomes more and more inaccurate for $\phi \gtrsim 1$. This is depicted in Fig. 1.10 for N_{\max} ranging from 3 to 10 and compared to the numerically evaluated full result. Note that increasing the number of expansion terms N_{\max} only improves the local quality of the approximation around $\phi = 0$ and would not help to improve the description of $\Gamma(\phi \gtrsim 1)$.

Mixed Scheme

After gaining the insight that the iteration scheme works well for $\phi \gtrsim 1$ and the vertex expansion is useful for $\phi \lesssim 1$ the idea to combine the advantages of both approximation schemes suggests itself. We therefore continue with the so called 'mixed scheme' in the following. For this purpose, we expand the effective average action as

$$\Gamma_R(\phi) = S(\phi) + \frac{1}{2} \ln \left(\partial_\phi^2 S(\phi) + R \right) + \sum_{n=0}^{N_{\max}} \frac{\lambda_{2n}}{(2n)!} \frac{\phi^{2n}}{(\partial_\phi^2 S(\phi) + R)^{2n+2}}. \tag{1.112}$$

While the first two terms compose the 1-loop effective average action, the third term resembles the vertex expansion for $\phi \ll 1$ and is suppressed as ϕ^{-4} for $\phi \gg 1$. The next step is now to project out the flow equations for the coefficients λ_{2n} and to solve these for different orders of the truncation by varying N_{\max} . The comparison with the full numerical solution is depicted in Fig. 1.11. The plot shows that the mixed-scheme effective action inherited tiny errors for $\phi \ll 1$ from the vertex expansion and for $\phi \gg 1$ from the loop expansion. However, the drawback of the mixed-scheme approximation becomes obvious when analyzing the convergence properties. Those are not under control, as one can see in Fig. 1.12. Including higher N_{\max} does not automatically lead to smaller errors. Therefore the scheme is not as convenient as hoped in the first place.

Remarkably, this shows already at the level of this simple zero-dimensional scalar theory that the discussion of the truncation error, as hard as it is, is very important within the FRG approach.

Figure 1.11: The error of the mixed-scheme approximation depending on ϕ for $N_{\max} = 1, 2, 3$.

Figure 1.12: The error of the mixed-scheme approximation depending on ϕ for $N_{\max} = 4, 5, 6$.

2 Appendix

2.1 Fourier Conventions

This appendix summarizes our Fourier conventions. In the following we denote bosonic fields with ϕ and fermionic fields with $\bar{\psi}$ and ψ . However the conventions are used for other fields, as e.g. bosonic vector fields A_μ , as well. The continuous Fourier transformation in one dimension reads

$$\begin{aligned}\phi(x) &= \int \frac{dp}{2\pi} \phi(p) e^{ipx}, & \psi(x) &= \int \frac{dp}{2\pi} \psi(p) e^{ipx}, & \bar{\psi}(x) &= \int \frac{dp}{2\pi} \bar{\psi}(p) e^{-ipx}, & \int dx e^{-ipx} &= 2\pi \delta(p), \\ \phi(p) &= \int dx \phi(x) e^{-ipx}, & \psi(p) &= \int dx \psi(x) e^{-ipx}, & \bar{\psi}(p) &= \int dx \bar{\psi}(x) e^{ipx}, & \int \frac{dp}{2\pi} e^{ipx} &= \delta(x).\end{aligned}$$

The generalization to d dimensions is obvious.

In subsection ?? of chapter 1 the time direction is compactified in order to introduce finite temperature. In this case the discrete version of the above Fourier convention has to be used. It reads

$$\begin{aligned}\phi(x) &= \frac{1}{\beta} \sum_{n=-\infty}^{\infty} \phi_n e^{2\pi i n x / \beta}, & \psi(x) &= \frac{1}{\beta} \sum_{n=-\infty}^{\infty} \psi_n e^{2\pi i (n + \frac{1}{2}) x / \beta}, & \bar{\psi}(x) &= \frac{1}{\beta} \sum_{n=-\infty}^{\infty} \bar{\psi}_n e^{-2\pi i (n + \frac{1}{2}) x / \beta}, \\ \phi_n &= \int_0^\beta dx \phi(x) e^{-2\pi i n x / \beta}, & \psi_n &= \int_0^\beta dx \psi(x) e^{-2\pi i (n + \frac{1}{2}) x / \beta}, & \bar{\psi}_n &= \int_0^\beta dx \bar{\psi}(x) e^{2\pi i (n + \frac{1}{2}) x / \beta}.\end{aligned}$$

The corresponding delta distribution and Kronecker delta in turn are given as

$$\int_0^\beta dx e^{-2\pi i n x / \beta} = \beta \delta_{n,0}, \quad \frac{1}{\beta} \sum_{n=-\infty}^{\infty} e^{2\pi i n x / \beta} = \delta(x).$$

2.2 Wilsonian Renormalization for φ^4 theory

The goal of this appendix is the exemplary discussion of the Wilsonian renormalization at the example of the φ^4 theory with the classical action (1.32). To be precise we aim at the quantum correction to the φ^4 coupling, $\Delta\lambda$, which appeared in (1.59). For this purpose we need $S_{\Lambda'}$ which follows from (1.58) as

$$S_{\Lambda'}[\tilde{\varphi}] = -\ln \left\{ \int_{\Lambda} [d\hat{\varphi}] \exp \left[-S_{\Lambda}[\tilde{\varphi}, \hat{\varphi}] + \int \frac{d^d p}{(2\pi)^d} \hat{\varphi}(p) J(-p) \right] \right\} \quad (2.1)$$

with the hard and soft modes, $\hat{\varphi}$ and $\tilde{\varphi}$ defined in (1.56). The split into hard and soft modes within the classical action S_{Λ} leads to

$$\begin{aligned}S_{\Lambda}[\tilde{\varphi}, \hat{\varphi}] &= S_{\Lambda}[\tilde{\varphi} + \hat{\varphi}] = S_{\Lambda}[\tilde{\varphi}] + S_{\Lambda}[\hat{\varphi}] + S_{\text{mix}}[\tilde{\varphi}, \hat{\varphi}] \\ S_{\text{mix}}[\tilde{\varphi}, \hat{\varphi}] &= \int \frac{d^d p_1}{(2\pi)^d} \int \frac{d^d p_2}{(2\pi)^d} \int \frac{d^d p_3}{(2\pi)^d} \left(\frac{\lambda}{3!} \hat{\varphi}(p_1) \tilde{\varphi}(p_2) \tilde{\varphi}(p_3) \tilde{\varphi}(-p_1 - p_2 - p_3) \right. \\ &\quad \left. + \frac{\lambda}{3!} \hat{\varphi}(p_1) \hat{\varphi}(p_2) \hat{\varphi}(p_3) \tilde{\varphi}(-p_1 - p_2 - p_3) + \frac{\lambda}{4} \hat{\varphi}(p_1) \hat{\varphi}(p_2) \tilde{\varphi}(p_3) \tilde{\varphi}(-p_1 - p_2 - p_3) \right).\end{aligned} \quad (2.2)$$

With this we find $S_{\Lambda'}[\tilde{\varphi}] = S_{\Lambda}[\tilde{\varphi}] + \Delta S[\tilde{\varphi}]$ with the quantum corrections due to the hard modes encoded in

$$\Delta S[\tilde{\varphi}] = -\ln \left\{ \int_{\Lambda} [d\hat{\varphi}] \exp \left[-S_{\Lambda}[\hat{\varphi}] - S_{\text{mix}}[\tilde{\varphi}, \hat{\varphi}] + \int \frac{d^d p}{(2\pi)^d} \hat{\varphi}(p) J(-p) \right] \right\}. \quad (2.3)$$

In order to find the correction to the φ^4 coupling we expand this expression in powers of $\tilde{\varphi}$ and for the sake of comparability to subsection 1.3.1 restrict ourselves to lowest order in λ . We find the four contributions

$$\begin{aligned} \Delta S|_{\tilde{\varphi}^4} = & \int \frac{d^d p_1}{(2\pi)^d} \int \frac{d^d p_2}{(2\pi)^d} \int \frac{d^d p_3}{(2\pi)^d} \int \frac{d^d q_1}{(2\pi)^d} \int \frac{d^d q_2}{(2\pi)^d} \int \frac{d^d q_3}{(2\pi)^d} \left(\right. \\ & -\frac{\lambda^2}{36} \tilde{\varphi}(p_2) \tilde{\varphi}(p_3) \tilde{\varphi}(-p_1 - p_2 - p_3) \tilde{\varphi}(-q_1 - q_2 - q_3) \langle \hat{\varphi}(p_1) \hat{\varphi}(q_1) \hat{\varphi}(q_2) \hat{\varphi}(q_3) \rangle \\ & \frac{\lambda^2}{36} \tilde{\varphi}(p_2) \tilde{\varphi}(p_3) \tilde{\varphi}(-p_1 - p_2 - p_3) \tilde{\varphi}(-q_1 - q_2 - q_3) \langle \hat{\varphi}(p_1) \rangle \langle \hat{\varphi}(q_1) \hat{\varphi}(q_2) \hat{\varphi}(q_3) \rangle \\ & -\frac{\lambda^2}{32} \tilde{\varphi}(p_3) \tilde{\varphi}(-p_1 - p_2 - p_3) \tilde{\varphi}(q_3) \tilde{\varphi}(-q_1 - q_2 - q_3) \langle \hat{\varphi}(p_1) \hat{\varphi}(p_2) \hat{\varphi}(q_1) \hat{\varphi}(q_2) \rangle \\ & \left. +\frac{\lambda^2}{32} \tilde{\varphi}(p_3) \tilde{\varphi}(-p_1 - p_2 - p_3) \tilde{\varphi}(q_3) \tilde{\varphi}(-q_1 - q_2 - q_3) \langle \hat{\varphi}(p_1) \hat{\varphi}(p_2) \rangle \langle \hat{\varphi}(q_1) \hat{\varphi}(q_2) \rangle \right) \quad (2.4) \end{aligned}$$

where one should keep in mind that the integrations with respect to the momenta of the hard modes $\hat{\varphi}$ are restricted to the momentum shell. Inserting the expectation values

$$\begin{aligned} \langle \hat{\varphi}(p_1) \hat{\varphi}(p_2) \rangle &= \frac{1}{p_1^2} (2\pi)^d \delta^{(d)}(p_1 + p_2), \\ \langle \hat{\varphi}(p_1) \hat{\varphi}(p_2) \hat{\varphi}(p_3) \rangle &= 0, \\ \langle \hat{\varphi}(p_1) \hat{\varphi}(p_2) \hat{\varphi}(p_3) \hat{\varphi}(p_4) \rangle &= \frac{1}{p_1^2 p_2^2} (2\pi)^d \delta^{(d)}(p_1 + p_4) (2\pi)^d \delta^{(d)}(p_2 + p_3) \\ &+ \frac{1}{p_1^2 p_3^2} (2\pi)^d \delta^{(d)}(p_1 + p_2) (2\pi)^d \delta^{(d)}(p_3 + p_4) \\ &+ \frac{1}{p_1^2 p_4^2} (2\pi)^d \delta^{(d)}(p_1 + p_3) (2\pi)^d \delta^{(d)}(p_2 + p_4) \quad (2.5) \end{aligned}$$

we find

$$\begin{aligned} \Delta S|_{\tilde{\varphi}^4} = & -\frac{\lambda^2}{16} \int \frac{d^d \hat{p}_1}{(2\pi)^d} \int \frac{d^d \hat{p}_2}{(2\pi)^d} \int \frac{d^d p_3}{(2\pi)^d} \int \frac{d^d q_3}{(2\pi)^d} \frac{1}{\hat{p}_1^2} \frac{1}{\hat{p}_2^2} \tilde{\varphi}(p_3) \tilde{\varphi}(q_3) \tilde{\varphi}(-\hat{p}_1 - \hat{p}_2 - p_3) \tilde{\varphi}(\hat{p}_1 + \hat{p}_2 - q_3) \\ & -\frac{\lambda^2}{12} \int \frac{d^d \hat{p}_1}{(2\pi)^d} \int \frac{d^d p_2}{(2\pi)^d} \int \frac{d^d p_3}{(2\pi)^d} \int \frac{d^d \hat{q}_3}{(2\pi)^d} \frac{1}{\hat{p}_1^2} \frac{1}{\hat{q}_3^2} \tilde{\varphi}(\hat{p}_1) \tilde{\varphi}(p_2) \tilde{\varphi}(p_3) \tilde{\varphi}(-\hat{p}_1 - p_2 - p_3). \quad (2.6) \end{aligned}$$

Here we indicate the integration restricted to the momentum shell by denoting the corresponding integration variables with a hat. The second contribution is depicted in Fig. 2.1 and illustrates again the fact that the Wilsonian effective action is not an effective action in the sense that it contains 1-particle reducible contributions. However, this specific contribution vanishes since $\tilde{\varphi}(\hat{p}_1) = 0$ by definition (1.56). The first line on the other hand describes a contribution which is reminiscent of the results obtained in the previous subsection and corresponds to the second diagram in the second line of Fig. 1.3 with momenta of the momentum shell running in the loop. Taking four derivatives of this contribution with respect to $\tilde{\varphi}$

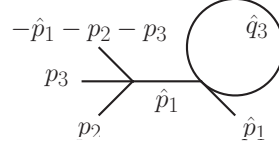


Figure 2.1: 1-particle reducible contribution to $\Delta\lambda$.

one finds the same quantum correction as in (1.36) but with the integration restricted to the momentum shell. To be precise we find

$$\frac{\delta^4 \Delta S|_{\tilde{\varphi}^4}}{\delta\tilde{\varphi}(Q_1)\delta\tilde{\varphi}(Q_2)\delta\tilde{\varphi}(Q_3)\delta\tilde{\varphi}(Q_4)} = \Delta\lambda = \quad (2.7)$$

$$-\frac{\lambda^2}{2}(2\pi)^d \delta^d\left(\sum_i Q_i\right) \int \frac{d^d \hat{p}}{(2\pi)^d} \left\{ \frac{1}{\hat{p}^2} \left[\frac{1}{(\hat{p} + Q_1 + Q_2)^2} + \frac{1}{(\hat{p} + Q_1 + Q_3)^2} + \frac{1}{(\hat{p} + Q_1 + Q_4)^2} \right] \right\}$$

where we are suppressing for notational convenience a theta function restricting $\hat{p} + Q_i + Q_j$ to the momentum shell with (i, j) being $(1, 2)$, $(1, 3)$ and $(1, 4)$ in the first, second and third contribution respectively.

2.3 Local Potential Approximation of the $O(N)$ Model

This appendix is devoted to the local potential approximation (LPA) introduced in section 1.5. We illustrate the analysis of the effective potential within the FRG framework at the example of a scalar $O(N)$ -symmetric theory. The effective average action Γ_k within this theory depends on N scalar fields ϕ^a with the index $a \in \{1, 2, \dots, N\}$. Its simplest truncation within the derivative expansion is the LPA and contains a scale-independent kinetic term and a scale-dependent effective average potential V_k . It reads

$$\Gamma_k[\phi^a] = \frac{1}{2} \int d^d x (\partial_\mu \phi^a)^2 + \int d^d x V_k \left[\frac{\phi^a \phi^a}{2} \right], \quad (2.8)$$

Note that due to the $O(N)$ symmetry the effective average potential depends on the squared fields. As discussed in section 1.5 with constant fields ϕ^a the 1PI effective average action reduces to a product of the effective average potential and a spacetime-volume factor. The latter one is the integral over the d -dimensional volume and can easily be performed. In the following it shall be considered as a prefactor Vol_d

$$\Gamma_k[\rho] = \text{Vol}_d \cdot V_k[\rho]. \quad (2.9)$$

Here we denote the square of the fields as $\rho = \frac{\phi^a \phi^a}{2}$. Although this effective potential has to be $O(N)$ symmetric its ground state does not. Let us clarify this with a simple example. Expanding the potential as

$$V_k = -\mu_k^2 \rho + \lambda_k \rho^2, \quad (2.10)$$

with k -dependent couplings μ_k^2 and λ_k . The minimum of this potential is situated at the origin if μ_k^2 is negative but might as well be situated at some finite value ρ_{\min} if μ_k^2 is positive. This corresponds to the upper right and left panels in Fig. 1.9 respectively. Thus for positive μ_k^2 , the ground state breaks the

$O(N)$ symmetry although the potential itself is symmetric. This effect is called spontaneous symmetry breaking (SSB). Now one might ask the question how the effective potential $V_{k \rightarrow 0}$, including all quantum fluctuations, looks like if we start at the classical level in the symmetric or the spontaneously broken phase of the potential. For this discussion the flow equation is an effective tool and we will investigate its application to the effective average potential in the following.

In order to find the flow equation for the effective potential we can evaluate the flow equation for the 1PI effective average action (1.83) with constant fields as explained in section 1.5. Thus we find

$$\partial_t \Gamma_k(\rho) = \text{Vol}_d \cdot \partial_t V_k(\rho). \quad (2.11)$$

To evaluate the right hand side of the flow equation (1.83) we need the second variation of the effective average potential with respect to the fields. It reads

$$\frac{\delta}{\delta \phi^a} \frac{\delta}{\delta \phi^b} V_k(\rho) = \delta^{ab} V'_k(\rho) + \phi^a \phi^b V''_k(\rho). \quad (2.12)$$

Here the prime denotes the derivative with respect to the argument ρ . This second derivative can be inserted into the right hand side of the flow equation. Evaluating the trace in field space while assuming a regulator diagonal in field space we obtain the flow equation for the effective, k -dependent potential. The resulting expression in momentum space reads

$$\partial_t V_k(\rho) = \frac{1}{2} \int \frac{d^d p}{(2\pi)^d} \left[\frac{N-1}{p^2 + V'_k(\rho) + R_k(p^2)} + \frac{1}{p^2 + V'_k(\rho) + 2\rho V''_k(\rho) + R_k(p^2)} \right] \partial_t R_k(p^2). \quad (2.13)$$

Here, the second term on the right hand side corresponds to the contribution of the radial mode (Higgs mode) in the mexican-hat type potential. The first contribution on the other hand describes the fluctuation of the Goldstone modes. This becomes obvious if we investigate the flow equation at the minimum of the potential. Then, by definition V' vanishes and the propagator in the first contribution becomes massless (up to the regulator). On the other hand the propagator of the second contribution has a mass $2\rho V''$ due to the Higgs mechanism.

There is one ingredient on the right hand side of (2.13) which we did not specify yet, the regulator R_k . In section ?? we discuss in detail how the choice of the regulator can be optimized. To anticipate the result of this section we introduce the optimized cutoff function as proposed by Litim [28, 29] here. The details about the optimization procedure shall be postponed for the moment. Explicitly the Litim cutoff reads

$$R_{k,\text{flat}}(p^2) = (k^2 - p^2) \Theta(k^2 - p^2), \quad (2.14)$$

with Θ being the theta function. Since the integrand of our flow equation depends only on the square of the momentum p we can rewrite the d -dimensional momentum integral as the unit $(d-1)$ -sphere Ω_d times a radial integration. The special form of the optimized cutoff then allows us to evaluate this radial integration analytically to finally find

$$\partial_t V_k(\rho) = \frac{\Omega_d}{(2\pi)^d} \frac{1}{d} k^{2+d} \left(\frac{N-1}{k^2 + V'_k(\rho)} + \frac{1}{k^2 + V'_k(\rho) + 2\rho V''_k(\rho)} \right). \quad (2.15)$$

This flow equation can be solved by a straightforward numerical implementation. However, if we restrict ourselves to the large- N approximation even an analytical solution is possible as we shall show in the following.

In order to get a hand on the large- N limit we rewrite the flow equation in a more convenient way. We absorb the $(N-1)$ dependence of (2.15) into the definition of the potential V_k and the squared field ρ , by

the corresponding redefinitions. In turn the second term in (2.15) can be neglected for large N . We find

$$\left. \begin{array}{l} V_k \rightarrow (N-1)V_k, \\ \rho \rightarrow (N-1)\rho, \end{array} \right\} \Rightarrow V'_k \rightarrow V'_k, \quad \Rightarrow \quad \partial_t V_k(\rho) \approx \frac{k^d}{d} \frac{\Omega_d}{(2\pi)^d} \frac{1}{1 + \frac{V'_k(\rho)}{k^2}}. \quad (2.16)$$

The appearance of the terms with k^2 and k^d impose a redefinition in terms of dimensionless quantities. Therefore, we now apply a further rescaling of the involved fields according to

$$\bar{\rho} = \frac{\rho}{k^{d-2}}, \quad u_k(\bar{\rho}) = \frac{V_k(k^{d-2}\bar{\rho})}{k^d} \quad \Rightarrow \quad \partial_t|_{\rho} \bar{\rho} = (2-d)\bar{\rho}. \quad (2.17)$$

Note that in the following it is important that the field ϕ and correspondingly ρ are the k -independent quantities. Consequently the dimensionless quantity $\bar{\rho}$ becomes k dependent according to (2.17). Next we evaluate the t -derivative of the dimensionless potential u_k twice using (2.17) and (2.16) respectively. For convenience we explicitly write down which quantity is kept fixed for the derivative in order to clarify the dependencies.

$$\begin{aligned} \partial_t|_{\rho} u_k(\bar{\rho}) &= \partial_t|_{\bar{\rho}} u_k(\bar{\rho}) + (2-d)\bar{\rho} u'_k(\bar{\rho}), \\ \partial_t|_{\rho} u_k(\bar{\rho}) &= \partial_t|_{\rho} \frac{V_k(\rho)}{k^d} = \frac{\partial_t|_{\rho} V_k(\rho)}{k^d} - d u_k(\bar{\rho}). \end{aligned} \quad (2.18)$$

What we are finally interested in is the first term on the right hand side of the first line. Comparing the two right hand sides and using the flow equation for $\partial_t|_{\rho} V_k$, (2.16), we arrive at the flow equation for the dimensionless potential u_k which reads

$$\partial_t u_k(\bar{\rho}) + d u_k(\bar{\rho}) + (2-d)\bar{\rho} u'_k(\bar{\rho}) = \frac{1}{d} \frac{\Omega_d}{(2\pi)^d} \frac{1}{1 + u'_k(\bar{\rho})}, \quad (2.19)$$

and depends on the potential u_k itself and its derivatives.

In order to solve this flow equation, it is useful to perform a derivative with respect to $\bar{\rho}$. In this way, we eliminate the potential's off-set. As a byproduct, it transform the equation into a form suitable for the method of characteristics as a solution strategy. Considering this, we end up with the flow equation for the potential's derivative $\omega_k(\bar{\rho}) = u'_k(\bar{\rho})$

$$0 = \partial_t \omega(\bar{\rho}) + 2\omega(\bar{\rho}) + (2-d)\bar{\rho} \omega'(\bar{\rho}) + \frac{1}{d} \frac{\Omega_d}{(2\pi)^d} \frac{\omega'(\bar{\rho})}{(1 + \omega(\bar{\rho}))^2}. \quad (2.20)$$

Here and in the following we suppress the index k of ω for better readability. In order to solve this partial differential equation (PDE) we use the method of characteristics. Thus, the goal is to transform the PDE into a system of ordinary differential equations (ODEs). The solution of the simplified ODEs subsequently allows for a construction of the PDE's solution. To this aim we firstly rewrite the non-linear PDE (2.20) in the form

$$a(t, \bar{\rho}, \omega) \partial_t \omega + b(t, \bar{\rho}, \omega) \partial_{\bar{\rho}} \omega - c(t, \bar{\rho}, \omega) = 0, \quad (2.21)$$

with coefficient functions a, b and c . To actually obtain the set of ODEs, we perform a coordinate transformation $t \rightarrow t(s, r)$ and $\bar{\rho} \rightarrow \bar{\rho}(s, r)$. With this parametrization (2.21) can be rewritten as

$$\frac{d}{ds} \omega(t(s), \bar{\rho}(s)) = c, \quad \text{if} \quad \frac{dt}{ds} = a, \quad \frac{d\bar{\rho}}{ds} = b \quad (2.22)$$

and the second coordinate r can be used to specify the initial condition.

To clarify this let us proceed with our specific example. For a function ω that obeys (2.20), we can identify the coefficient functions a, b and c by comparison with (2.21) as

$$\begin{aligned} a(t, \bar{\rho}, \omega) &= 1 \\ b(t, \bar{\rho}, \omega) &= (2-d)\bar{\rho} + \underbrace{\frac{1}{d} \frac{\Omega_d}{(2\pi)^d}}_{=A} \frac{1}{(1+\omega)^2} \\ c(t, \bar{\rho}, \omega) &= -2\omega, \end{aligned} \quad (2.23)$$

with the shorthand A as indicated by the underbrace. From the second ODE in (2.22) we thus find $t(s) = s$ where we specified for a vanishing constant of integration. Bearing in mind the picture of scale dependent quantities we recall that the initial condition for the flow equation (2.20) are set at a UV scale $k = \Lambda$ ($t = 0$ for $t = \log(k/\Lambda)$) where we can choose a classical potential. In combination with the solution of the first ODE above this specifies $s_{\text{ini}} = 0$. With this we are left with the two ODEs

$$\frac{d\omega}{ds} = -2\omega, \quad \frac{d\bar{\rho}}{ds} = (2-d)\bar{\rho} + \frac{A}{(1+\omega)^2} \quad (2.24)$$

and the initial condition $\bar{\rho}(s=0) = \bar{\rho}_0$ and $\omega(0, \bar{\rho}_0)$ chosen as the classical potential's derivative. If we now vary $\bar{\rho}_0$ we find $\omega(s)$ along the so-called corresponding characteristic curves parameterized by s and specified by $\bar{\rho}_0$. The solutions along all curves put together finally give us $\omega(t = s, \bar{\rho}(s, \bar{\rho}_0))$. Denoting the initial potential's derivative as ω_0 we find the following solution for ω

$$\omega(s) = \omega_0 \exp(-2s). \quad (2.25)$$

The solution to (2.24) for $\bar{\rho}$ reads

$$\bar{\rho}(s) = \bar{\rho}_0 + \int_0^s ds' \left((2-d)\bar{\rho}(s') + \frac{A}{(1+\omega_0 e^{-2s'})^2} \right). \quad (2.26)$$

This solution can be interpreted as the initial $\bar{\rho}_0$ as a function of $\bar{\rho}$ which shall be inserted into the result for the potentials derivative (2.25) where the initial potential's derivative should be interpreted as $\omega_0(\bar{\rho}_0(\bar{\rho}))$. Subsequently, we get $\omega(t, \bar{\rho}(t))$ where we used the identification $t = s$ from the solution of the first ODE. This represents the solution to (2.20).

Before inspecting the full Potential and its scale dependence let us concentrate on its minimum. The latter contains the relevant information for the description of spontaneous symmetry breaking and thus it is worth discussing its flow separately. Inspecting again the ODE for $\bar{\rho}$ in (2.24) we can identify the corresponding ODE for the dimensionful ρ . The corresponding ODE and its solution read

$$\begin{aligned} \frac{d\rho}{ds} &= \Lambda^{d-2} e^{(d-2)s} \frac{A}{(1+\omega_0 e^{-2s})^2}, \\ \rho(s) &= \rho_0 + \int_0^s ds' \frac{\Lambda^{d-2} e^{(d-2)s'} A}{(1+\omega_0 e^{-2s'})^2}. \end{aligned} \quad (2.27)$$

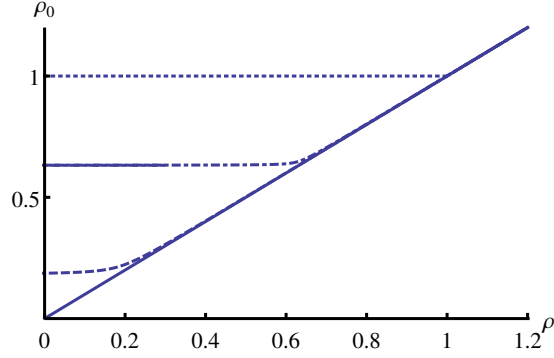


Figure 2.2: Depicted is the initial ρ_0 depending on ρ for $s = 0$ (solid line), $s = -0.1$ (dashed line), $s = -0.5$ (dash-dot line) and $s = -\infty$ (dotted line). The scale is set by choosing $\Lambda = 1$ and as the initial potential a quadratic one is chosen as in (2.10) with $\lambda_\Lambda = 0.5$ and $\mu_\Lambda = 1$.

Again we can interpret the solution as the initial ρ_0 depending on ρ . For illustrative purposes this dependence is depicted in Fig. 2.2. This plot was obtained in $d = 4$ with a quadratic initial potential at $k = \Lambda$ as in (2.10). One can see the straight line $\rho_0 = \rho$ which is given for $s = t = 0$. For decreasing s the value of ρ_0 increases since the integral on the right hand side of (2.27) is negative for negative s . For $s \rightarrow -\infty$ ($k \rightarrow 0$) a plateau at $\bar{\rho}_0 = 1$ establishes. This will help us during the discussion of the evolution of the potential below. However, first a further analysis of the the scale dependent ρ is in order.

Now we are in the position to discuss the potential's minimum to see whether it is trivial (symmetric phase) or non-trivial (broken phase). Its location is determined by $\omega(\bar{\rho}) = \partial_{\bar{\rho}} u(\bar{\rho}) = 0$. According to (2.25) we thus need $\omega_0 = 0$ which upon insertion into (2.27) leads to

$$\rho_{\min}(t) = \rho_{0,\min} + \frac{A \Lambda^{d-2}}{d-2} \left(e^{(d-2)t} - 1 \right). \quad (2.28)$$

Here it is important to point to the denominator $(d-2)$. It marks the peculiarity of the case $d = 2$ which is the topic of the Mermin-Wagner theorem [30, 31]. The latter states that there is no continuous phase transition in two-dimensional systems with continuous symmetries. For a detailed study of this issue within the FRG framework see [32]. To circumvent this subtlety we will stick to dimensions $d > 2$ in the following. The interpretation of (2.28) is then as follows. Starting at some high energy scale $k = \Lambda$ corresponding to $t = 0$ we can evolve our system towards low energies at negative t . Eq. (2.28) then shows that if the initial potential is in the spontaneously broken phase ($\rho_{0,\min} > 0$) its minimum decreases, as the second term in (2.28) turns negative. If, on the other hand, the initial potential is in the symmetric phase ($\rho_{0,\min} = 0$) it stays in the symmetric phase during the k evolution, see the right plots in Fig. 1.9. Integrating down to $k = 0$, corresponding to $t \rightarrow -\infty$, where the effective average action is equal to the 1PI effective action, we find

$$\rho_{\min}(k = 0) = \rho_{0,\min} - \frac{\Lambda^{d-2} A}{d-2}. \quad (2.29)$$

Specifying the initial potential to the example (2.10) we find $\rho_{0,\min} = \mu_\Lambda^2 / (2\lambda_\Lambda)$. If we now fix the value of λ_Λ and vary μ_Λ in $\rho_{0,\min}$ we find a second order phase transition in ρ_{\min} as a function of μ_Λ^2 , as illustrated in Fig. 2.3 with a blue line. In other theories different from the simple scalar example we are discussing here it might be possible to find as well a first order phase transition which would look like the red line in Fig. 2.3.

Next we can discuss the scale evolution of the potential's derivative and the potential itself. Starting with the derivative we have to investigate the solution (2.25) where we have to insert the $\bar{\rho}$ dependent $\bar{\rho}_0$ given

in (2.26) and depicted in Fig. 2.2 for its dimensionful counterpart. For $k \rightarrow 0$ this plot shows that $\bar{\rho}_0$ becomes independent of $\bar{\rho}$ for small values of $\bar{\rho}$. Therefore ω is independent of $\bar{\rho}$ and the exponential damping in (2.25) results in $\omega \approx 0$ for an extended range of $\bar{\rho}$ values. This translates into a constant potential as it is depicted in the lower left plot of Fig. 1.9. This makes the effective potential convex as we expected according to our discussion in section 1.5.

The qualitative behavior of the (dimensionless) potential's flow in momentum space is shown in Fig. 2.4, where the evolution of the k -scale shifts the minima towards the origin.

In order to investigate the flow of the minimum of the actual potential, $\partial_\rho V_k|_{\rho_{\min}}$, we re-introduce dimensionful quantities with the help of (2.17). The flow equation (2.24) for the dimensionless $\bar{\rho}$ then leads to the following dimensionful version at the minimum

$$\partial_t \rho_{\min} = k^{d-2} A. \quad (2.30)$$

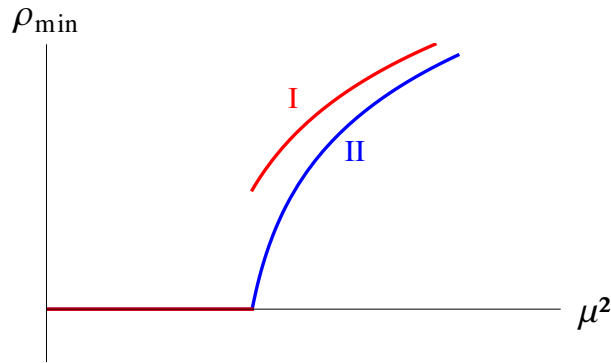


Figure 2.3: First and second order phase transitions in ρ_{\min} under variation of the coupling μ^2 .

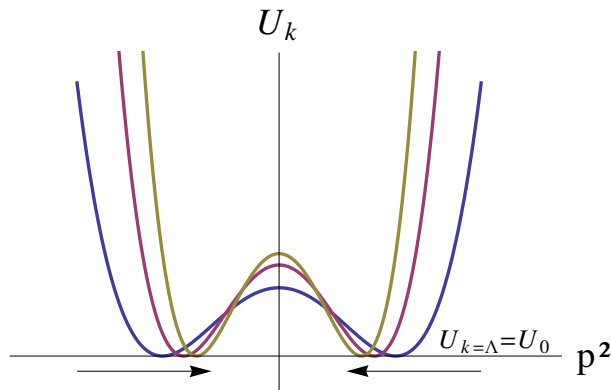


Figure 2.4: The flow of the effective potential u_k under variation of cutoff scale k if t is negative.

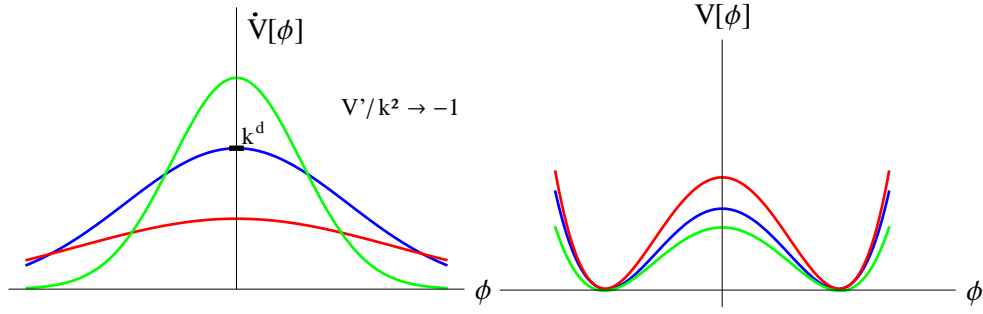


Figure 2.5: The flow of the k -derivative of the effective potential in the limit $V'/k^2 \rightarrow -1$.

Note that the corresponding solution is already given in (2.28). Using this flow equation we find the flow equation for the dimensionful potential's derivative to be

$$\begin{aligned}
 0 &= \partial_t \left(\partial_\rho V_k |_{\rho_{\min}} \right) = \partial_t \partial_\rho V_k |_{\rho_{\min}} + \partial_\rho^2 V_k |_{\rho_{\min}} \partial_t \rho_{\min} , \\
 &\Rightarrow \partial_t V'_k(\rho_{\min}) = -V''_k(\rho_{\min}) k^{d-2} A .
 \end{aligned} \tag{2.31}$$

The dimensionful potential V , illustrated in Fig. 2.5, shows that the introduction of quantum fluctuations during the evolution of the k -scale wash out the sharpness of the phase transition between $O(N)$ -symmetric and $O(N)$ -broken phase. This can already be seen from the flattening of the (non-convexity of the) potential V_k on the right hand side and its derivative on the left hand side of Fig. 2.5.

However, returning to the minima of the potential, the integration of (2.28) yields

$$\bar{\rho}_{\min} = \bar{\rho}_{0,\min} - \frac{1}{d-2} A (1 - \exp((d-2)t)) . \tag{2.32}$$

2.4 Grassmann variables: Reminder

Fermionic fields are described by Grassmann variables which are anticommuting numbers. Thus for two Grassmann variables c_1 and c_2 the anticommutator vanishes

$$\{c_1, c_2\} = 0 . \tag{2.33}$$

It follows directly that $c_1^2 = c_2^2 = 0$ and thus any function of Grassmann variables is given by an expansion

$$f(c) = f(0) + \frac{d}{dc} f(0) c . \tag{2.34}$$

The integration is defined by

$$\int dc 1 = 0, \quad \int dc c = 1 \quad \Rightarrow \quad \int dc f(c) = \frac{d}{dc} f(0) . \tag{2.35}$$

The formulation can be extended straightforward to complex Grassmann variables by introducing

$$c = \frac{1}{\sqrt{2}} (c_1 + ic_2) , \quad \bar{c} = \frac{1}{\sqrt{2}} (c_1 - ic_2) \tag{2.36}$$

with real Grassmann variables c_1 and c_2 . It follows immediately that $\bar{c}c = -c\bar{c}$.

Now let us use N -dimensional vectors of complex Grassmann variables, c_i and c_j . It is easily shown that for a unitary transformation $c'_i = U_{ij}c_j$ the product of complex Grassmann variables transforms as $\prod_i c'_i = (\det U) \prod_i c_i$. Therefore, the integral $\prod_i \int d\bar{c}_i dc_i$ is invariant under such unitary transformations. With this it is straightforward to evaluate a Gaussian integral which involves a Hermitian matrix M_{ij} with eigenvalues denoted by m_i :

$$\begin{aligned} \prod_{n=1}^N \int d\bar{c}_n dc_n \exp\left(-\sum_{i,j} \bar{c}_i M_{ij} c_j\right) &= \prod_{n=1}^N \int d\bar{c}_n dc_n \exp\left(-\sum_i \bar{c}_i m_i c_i\right) \\ &= \prod_{n=1}^N \int d\bar{c}_n dc_n \left(1 - \sum_i \bar{c}_i m_i c_i\right) = \det M. \end{aligned} \quad (2.37)$$

In the first line we used a unitary transformation to diagonalize M . In the second line we used (2.34) and (2.35). Notice that for ordinary variables the Gaussian integral would be proportional to the square root of the inverse determinant.

2.5 Flow equation of a four-Fermi coupling

The aim of this appendix is to derive the flow equation for the four-Fermi coupling of a simple ansatz reminiscent of the Nambu–Jona-Lasinio model. This ansatz reads

$$\Gamma_k = \int d^4x \left\{ \bar{\psi} i \not{\partial} \psi + \frac{g_k}{2} (\bar{\psi} \psi)^2 \right\}. \quad (2.38)$$

Inserting it into the Wetterich equation (??) and evaluating the result on a constant background, $\bar{\psi}(x), \psi(x) = \text{const.}$, we find the left hand side to be

$$\partial_t \Gamma_k = \frac{\text{Vol}_4}{2} \partial_t g_k (\bar{\psi} \psi)^2. \quad (2.39)$$

A comparison of this with the right hand side evaluated below allows for the extraction of the flow equation for g_k by a comparison of the field monomials.

Next we can go for the right hand side. With the fermionic regulator insertion as given in (??) we find the full, inverse propagator $\Gamma_k^{(2)} + R_k = \mathcal{P} + \mathcal{F}$ with its propagator part \mathcal{P} and its fluctuation part \mathcal{F} . The latter is given as

$$\begin{aligned} \mathcal{F} &= \begin{pmatrix} \mathcal{F}_{11} & \mathcal{F}_{12} \\ \mathcal{F}_{21} & \mathcal{F}_{22} \end{pmatrix} \quad \text{with} \quad \mathcal{F}_{11} = -g_k [\bar{\psi}^T \bar{\psi}], \\ &\quad \mathcal{F}_{12} = -g_k [\bar{\psi} \psi + \psi \bar{\psi}]^T = -\mathcal{F}_{21}^T, \\ &\quad \mathcal{F}_{22} = -g_k [\psi \psi^T] \end{aligned} \quad (2.40)$$

on the constant background, $\bar{\psi}(x), \psi(x) = \text{const.}$, while the former reads

$$\begin{aligned} \mathcal{P}(p, q) &= \begin{pmatrix} 0 & -\not{p}^T (1 + r_k) \\ -\not{p} (1 + r_k) & 0 \end{pmatrix} (2\pi)^4 \delta^{(4)}(p - q) \\ \Rightarrow \mathcal{P}^{-1}(p, q) &= \begin{pmatrix} 0 & -\not{p} (1 + r_k) \\ -\not{p}^T (1 + r_k) & 0 \end{pmatrix} \frac{(2\pi)^4 \delta^{(4)}(p - q)}{p^2 (1 + r_k)^2}. \end{aligned} \quad (2.41)$$

Thus, we find the fluctuation part to be quadratic in the fermionic fields. Next, we can manipulate the right hand side of the Wetterich equation in order to compare the field monomials as suggested above.

With the minus sign for the fermions we write

$$\begin{aligned}\partial_t \Gamma_k &= -\frac{1}{2} \text{Tr} \frac{\partial_t R_k}{\Gamma_k^{(2)} + R_k} = -\frac{1}{2} \text{Tr} \tilde{\partial}_t \ln [\Gamma_k^{(2)} + R_k] = -\frac{1}{2} \text{Tr} \tilde{\partial}_t \ln [\mathcal{P} + \mathcal{F}] \\ &= \text{const.} - \frac{1}{2} \text{Tr} \tilde{\partial}_t \left[\mathcal{P}^{-1} \mathcal{F} - \frac{1}{2} (\mathcal{P}^{-1} \mathcal{F})^2 + \frac{1}{3} (\mathcal{P}^{-1} \mathcal{F})^3 + \dots \right]\end{aligned}\quad (2.42)$$

where we introduced the $\tilde{\partial}_t$ derivative which acts on R_k but not on $\Gamma_k^{(2)}$. Furthermore, we expanded the logarithm and the ellipses denote higher orders. Since the fluctuation matrix \mathcal{F} is quadratic in the fermionic fields and we are looking at the four-Fermi interaction it suffices to consider the second term in the last line:

$$\partial_t \Gamma_k |_{(\bar{\psi}\psi)^2} = \frac{1}{4} \text{Tr} \tilde{\partial}_t (\mathcal{P}^{-1} \mathcal{F})^2 = \frac{1}{2} \text{Tr} \tilde{\partial}_t (\mathcal{P}_{12}^{-1} \mathcal{F}_{22} \mathcal{P}_{21}^{-1} \mathcal{F}_{11}) + \frac{1}{2} \text{Tr} \tilde{\partial}_t (\mathcal{P}_{12}^{-1} \mathcal{F}_{21} \mathcal{P}_{12}^{-1} \mathcal{F}_{21}). \quad (2.43)$$

The trace is a trace in momentum space as well as Dirac and field space. The latter one has been evaluated in the last step and the indices at \mathcal{P}^{-1} and \mathcal{F} are field-space indices. Starting with the first of the two terms we find

$$\frac{1}{2} \text{Tr} \tilde{\partial}_t (\mathcal{P}_{12}^{-1} \mathcal{F}_{22} \mathcal{P}_{21}^{-1} \mathcal{F}_{11}) = \frac{g_k^2 \text{Vol}_4}{2} \int \frac{d^4 p}{(2\pi)^4} \tilde{\partial}_t \frac{(1+r_k)^2}{[p^2(1+r_k)^2]^2} (\bar{\psi} \not{p} \psi)^2 \quad (2.44)$$

which is a four-Fermi term but does not have the expected Dirac structure. This is a new contribution, a vector contribution, which is generated during the flow. Here we will discard it since it is not contained in our truncation. However in general such terms should be considered and we will come back to this point in section ???. After discarding this contribution we can evaluate the second one. It reads

$$\frac{1}{2} \text{Tr} \tilde{\partial}_t (\mathcal{P}_{12}^{-1} \mathcal{F}_{21} \mathcal{P}_{12}^{-1} \mathcal{F}_{21}) = \frac{g_k^2 \text{Vol}_4}{2} \int \frac{d^4 p}{(2\pi)^4} \tilde{\partial}_t \frac{(1+r_k)^2}{[p^2(1+r_k)^2]^2} [2p^2 (\bar{\psi}\psi)^2 - (\bar{\psi} \not{p} \psi)^2] \quad (2.45)$$

where we find again vector contributions which we discard. The left over result can then be compared to the left hand side of the Wetterich equation to get the flow equation for the four-Fermi coupling, g_k . The result reads:

$$\partial_t g_k = 2g_k^2 \int \frac{d^4 p}{(2\pi)^4} \tilde{\partial}_t \frac{1}{p^2(1+r_k)^2}. \quad (2.46)$$

Bibliography

- [1] C. D. Roberts and A. G. Williams, *Prog. Part. Nucl. Phys.* **33**, 477 (1994), hep-ph/9403224.
- [2] R. Alkofer and L. von Smekal, *Phys. Rept.* **353**, 281 (2001), hep-ph/0007355.
- [3] C. D. Roberts and S. M. Schmidt, *Prog. Part. Nucl. Phys.* **45**, S1 (2000), nucl-th/0005064.
- [4] C. S. Fischer, *J.Phys.G* **G32**, R253 (2006), hep-ph/0605173.
- [5] D. Binosi and J. Papavassiliou, *Phys.Rept.* **479**, 1 (2009), 0909.2536.
- [6] J. M. Pawłowski, *Annals Phys.* **322**, 2831 (2007), hep-th/0512261.
- [7] J. Callan, Curtis G., *Phys.Rev.* **D2**, 1541 (1970).
- [8] K. Symanzik, *Springer Tracts Mod.Phys.* **57**, 222 (1971).
- [9] K. Symanzik, *Commun.Math.Phys.* **23**, 49 (1971).
- [10] I. Nandori, *JHEP* **04**, 150 (2013), 1208.5021.
- [11] C. Wetterich, *Phys.Lett.* **B301**, 90 (1993).
- [12] M. Bonini, M. D’Attanasio, and G. Marchesini, *Nucl. Phys.* **B409**, 441 (1993), hep-th/9301114.
- [13] U. Ellwanger, *Z. Phys.* **C62**, 503 (1994), hep-ph/9308260.
- [14] T. R. Morris, *Int. J. Mod. Phys.* **A9**, 2411 (1994), hep-ph/9308265.
- [15] C. Becchi, (1996), hep-th/9607188.
- [16] F. J. Wegner and A. Houghton, *Phys. Rev.* **A8**, 401 (1973).
- [17] S. Weinberg, *General Relativity: An Einstein centenary survey*, Eds. Hawking, S.W., Israel, W; Cambridge University Press , 790 (1979).
- [18] O. J. Rosten, (2010), 1003.1366.
- [19] C. Bervillier, (2014), 1405.0791.
- [20] D. F. Litim and J. M. Pawłowski, *Phys.Rev.* **D66**, 025030 (2002), hep-th/0202188.
- [21] T. Papenbrock and C. Wetterich, *Z.Phys.* **C65**, 519 (1995), hep-th/9403164.
- [22] M. Pernici and M. Raciti, *Nucl. Phys.* **B531**, 560 (1998), hep-th/9803212.
- [23] U. Ellwanger, *Z.Phys.* **C76**, 721 (1997), hep-ph/9702309.
- [24] A. Codello, M. Demmel, and O. Zanusso, (2013), 1310.7625.
- [25] J. Keitel and L. Bartosch, *J.Phys.* **A45**, 105401 (2012), 1109.3013.
- [26] S. Kemler and J. Braun, *J.Phys.* **G40**, 085105 (2013), 1304.1161.

- [27] S. Moroz, PhD Thesis (2011).
- [28] D. F. Litim, JHEP **0111**, 059 (2001), hep-th/0111159.
- [29] D. F. Litim, Phys. Rev. **D64**, 105007 (2001), hep-th/0103195.
- [30] N. Mermin and H. Wagner, Phys.Rev.Lett. **17**, 1133 (1966).
- [31] P. Hohenberg, Phys.Rev. **158**, 383 (1967).
- [32] A. Codello and G. D'Odorico, Phys.Rev.Lett. **110**, 141601 (2013), 1210.4037.